UNIVERSITY "POLITEHNICA" OF BUCHAREST

DOCTORAL SCHOOL OF APPLIED CHEMISTRY AND MATERIALS SCIENCE

DOCTORAL THESIS

SUMMARY

INNOVATIVE METHODS FOR DETECTING SPECIFIC BIOMARKERS OF CEREBRAL TUMORS

PhD Student: Sorin Sebastian Gheorghe

Coordinator: Prof. Dr. habil Raluca Ioana van Staden

BUCHAREST

2021

Keywords: sensor; cerebral tumors; biomarkers

The doctoral thesis" Innovative Methods for Detecting Specific Biomarkers of Cerebral Tumors" contains 127 pages, 8 chapters and cites 238 bibliographic references. The content of the paper in which the numbering of the pages of the thesis was kept is:

INTRODUCTION

Brain tumors are one of the most difficult pathologies, as they require a diagnosis as fast and close as possible to the beginning of the tumor development, a tumor ablation as complete as possible, without the patient being left with new postoperative sequelae ("maximal safe resection") and a careful postoperative follow-up to prevent tumor relapse. Most of the time, this process is not limited to just the neurosurgeon, but requires a whole team for the diagnosis (radiology, immunology, biochemistry, histopathology), treatment (neurosurgery, anesthesia and intensive care, radiotherapy, chemotherapy) and postoperative recovery and follow-up of the patient (neurology, psychiatry, medical recovery).

Stochastic sensors have many advantages in the study of tumor biomarkers, such as fast testing speed, reliability, considerably lower costs compared to classical tests and the possibility of conducting a quantitative and qualitative test simultaneously. In the future, these sensors will be widely used directly by the patient for the surveillance of the evolution of the brain tumor, similar to the testing of blood glucose levels by diabetic patients, but also for monitoring the state of health in general. The introduction of these sensors directly into the neurosurgeons' offices can be a real benefit for the minimally invasive diagnosis of brain tumors, the prognosis of the pathology and for the selection of the most effective therapeutic solutions.

That is why we have chosen as the main subject of the thesis the design, characterization and validation of 2D and 3D stochastic sensors used in the qualitative and quantitative analysis of some biomarkers of interest in the early diagnosis of brain tumors (dopamine, L-DOPA, hereguline α, IDH 1, IDH 2 and interleukins (IL6, 12 and β) obtained from different biological samples (blood, tissue, urine).

CHAPTER 1. BIOMARKERS USED FOR THE DIAGNOSIS OF BRAIN TUMORS

According to CBTRUS, in the US, between 2013 and 2017, 81,246 deaths were caused by primary malignant CNS tumors, representing an average annual mortality rate of 4.42 per 100,000 people and an average of 16,249 deaths per year from CNS malignant tumors [1].

Median survival in primary malignant CNS tumors was lowest for glioblastomas (8 months) and highest for malignant tumors of the pituitary gland (approx. 11.5 years). In a period of 5 years, out of the total patients diagnosed with primary malignant CNS tumors, only 23.5%

survived. The highest survival was in children aged 0 to 14 years (63.8%), compared to patients aged 15 to 39 years (59.1%) or over 40 years (12.8%) [1].

1.2. Classification of cerebral tumors

The first classification of brain tumors was made by Bailey and Cushing (1925) and started from the idea that they are of embryonic origin and comprised 14 categories. They concluded that tumors with differentiated cells evolve more slowly, even over the course of years in the case of oligodendroglyomas, while tumors with undifferentiated cells (e.g. polymorphic glioblastomas) show a higher degree of malignancy, have a faster evolution and relapse much more frequently. This classification was then simplified later by Bailey, reducing it to 10 categories by eliminating rarer forms. Although it has long been outdated, this classification is still useful in targeting treatment; based on this we know that radiation therapy is most effective in the case of young cell tumors [5].

Other classifications that made important contributions were the Kenohan et al. (1949) classification which introduced a standard system of 4 stages ranging from benign to malignant and the Zülch (1979) and Rubinstein (1982) classifications which encompassed all intracranial expansive processes and were the foundation of subsequent international classifications [2].

The first Romanian classification of brain tumors was made by Arseni and Carp (1978), dividing them into 3 categories [6]:

1. Tumors derived from embryonic remains, through defects of ontogenesis

2. Tumors derived from adult cells situated in the CNS

3. CNS tumors, localized in the brain or the rest of the organism

The histopathological classification of the primary CNS tumors is considered the classic classification and is the most commonly used one. This classification involves the microscopic identification of the cellular type and cellular changes, as well as the analysis of the tumor vascularization from the biopsy obtained intraoperatively. These data, along with clinical ones divide tumors into 2 categories: benign or malignant. It is important to note that although a tumor may be considered benign from a histopathological point of view, it can behave in a "malignant" way because of its location in eloquent or vital areas of the brain [2].

The most recent, most detailed and complete classification of primary CNS tumors is the fifth edition of the WHO classification of the tumors of the central nervous system (WHO CNS5). This is the sixth version of the international standard for classifying CNS tumors and adds new information over previous publications from 1979, 1993, 2000, 2007 and 2016. WHO CNS5 complements the fourth edition, which was published in 2016, when there were numerous scientific advances in the field of CNS oncology, including the use of the recommendations of The Consortium to Inform Molecular and Practical Approaches to CNS Tumor Taxonomy (cIMPACT-NOW). This 2021 version of the WHO classification brings significant updates by recognizing and advancing the understanding of the role of molecular diagnostics in the classification of primary CNS tumors [7].

1.3. Current methods for the diagnosis of cerebral tumors

Most brain tumors are diagnosed only after the onset of symptomatology.

The investigations that attest to the presence of the brain tumor are the following:

- Magnetic Resonance Imaging of the brain (cerebral MRI) - provides higher quality images than the Computer Tomography scan (CT-scan), with better resolution and is more specific to the nervous tissue than CT.
- Cerebral imaging with contrast substance (Intravenous Gadolinium for MRI and iodine substance for CT) allows for a more detailed view of the anatomic relations of the tumor with the neighboring structures and its characteristics, in turn suggesting the type of tumor present and in some cases even its degree of differentiation, before performing a biopsy.
- Cerebral imaging with angiography (angio-MRI, angio-CT) offers details about the relationship between the tumor and the cerebral vessels and the tumor`s vascularization
- MRI associated spectroscopy offers information about the chemical composition of the brain and helps in differentiating the necrotized tissue due to previous radiotherapy and the rest of the tumor
- Functional MRI is useful for appreciating the relationship of the tumor with cortical areas responsible for movement and speech and for presurgical planning so that those eloquent areas are protected and spared during surgical tumors ablation
- Biopsy – the positive diagnosis is offered by the histopathological examination of the tumor sample

- Cerebral computer tomography (cerebral CT) offers 3D images of the brain using X-rays. The cerebral CT can identify bleedings in the brain, the tumor and in the ventricular system as well as intracranial cerebral pathologies. The CT-scan is a type of investigation that can be done in case of patients that cannot undergo an MRI investigation (patients with pacemakers or non-ferromagnetic materials in the body).

- Cerebral Positron Emission Tomography (cerebral PET-CT) - used during the treatment of brain tumors, to differentiate the remaining tumor or new tumor tissue from therapeutically neutralized tumor tissue. It uses the property of metabolically active cells to absorb the substance used for this study.

- Cerebral angiography uses a contrast substance injected directly into a high-caliber artery and offers information of the cerebral vascularization and of the tumor vascularization

- Lumbar puncture can detect tumor cells present in the cerebrospinal fluid under microscopic examination or the presence of tumor biomarkers

- Molecular analysis of the tumors can identify genes, proteins and other cerebral tumor specific biomarkers. Some of those markers (biological markers or biomarkers) offer information regarding the patient`s prognosis and their probability of a positive response to a certain type of treatment plan

- Visual and auditory testing determines the degree in which the cerebral tumor affects the sensory functions

- Neurocognitive tests – testing the memory, attention, language, dexterity, ability to concentrate, the ability to perform calculations, in order to compare with future post-therapeutic results.

- Electroencephalography (EEG) is a non-invasive method that uses electrodes attached to the patient's head to measure the electrical activity of the brain, allowing the identification and monitoring of possible epileptic seizures.

- Monitoring of evoked potentials – uses electrodes to measure electrical activity of the nerves and can detect acoustic neuromas (posterior fossa brain tumors). It also serves to guide the resection of a tumor in relation to important nervous structures.

2.4.2. Construction of stochastic sensors

In the simplest example, the sensor has 2 states: occupied (by the analyte) and unoccupied. The 2 states produce different records. The stochastic sensor provides not only information about the concentration of the analyte, but also information about its specific structure, being most often enough to identify it. In Figure 2.2 we can see a single pore placed in a lipid plane that forms a bilayer. In an applied electrical potential, a current is conducted by the saline ions that surround both sides of the bilayer and passed through the pore. The pore contains the connecting site specially designed for the analyte, represented by the green ball in the figure. Each time the analyte binds to the pore, the current is modulated as illustrated at the bottom of the figure. Thus, this technique monitors individual binds of the pore with the analyte. The frequency of these events reveals the concentration of the analyte, while the current signature (the average of the duration and amplitude of the event) reveals the identity of the molecule.
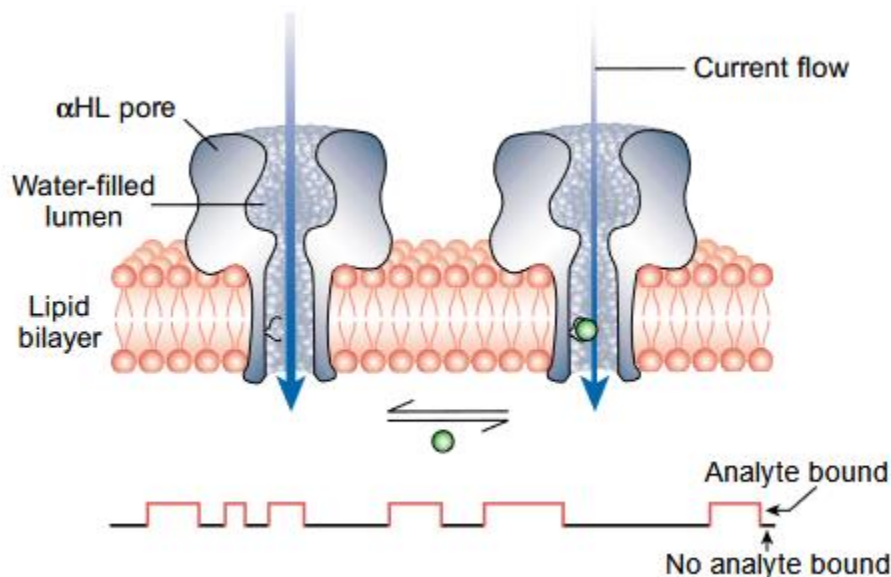
Figura 2.2. Current development in the stochastic sensor [109]

The pores used for stochastic detection are based on staphylococcal α-hemolysis (α-HL). The pore formed by the α-HL wild-type consists of 7 identical subunits arranged around a central axis. The transmembrane part of the lumen is a β domain with 2 antiparallel axes that each

contribute to the subunit. The extramembranous part contains a wide cavity that houses the transmembrane region during the assembly process, but which is available for synthesizing in the created pore. Although channels and pores have been used for some time to detect analytes [129,130], protein engineering and the detection of individual molecules have enormously increased the potential of this technology [131,132]. The 3D structure of the α-HL is known with high resolution and, most importantly, the β transmembrane domains are especially available for remodeling [133].

2.4.3. Advantages of stochastic sensors

Stochastic sensors can be used for the simultaneous detection of biomarkers in different biological samples, their response not being influenced by the analysis matrix. Stochastic sensors have a sensitivity and selectivity far above the classic (bio)sensors. These sensors are the only ones that can perform the qualitative and quantitative analysis of a biological sample with maximum reliability.

CHAPTER 3. DETECTION OF DOPAMINE AND L-DOPA FROM BLOOD AND TISSUE SAMPLES

3.2.2. Stochastic sensor design

For the design of the two 3D stochastic sensors, 10mg multi-walled carbon nanotube powder was mixed with 5μL of gold nanoparticles dispersion and 30μL paraffin oil until a homogeneous paste was obtained. In order to obtain the modified paste, 10μL solution of 1-adamantyloleamide (1.00×10^{-3} mol/L, prepared in ethanol) was used as chemical modifier in the design of the 3D stochastic sensor. Both types of paste: unmodified paste and modified paste with 1-adamantyloleamide were used for the design of the stochastic sensors. Each paste was placed in a 3D printed tube (3D printing was using aols non-conducting polymer) and a silver wire was used as electric contact between the paste and the external circuit (Figure 1). The sensors were cleaned with deionized water, and dried between two measurements. The active surface of each type of sensor was renewed by polishing on alumina paper.
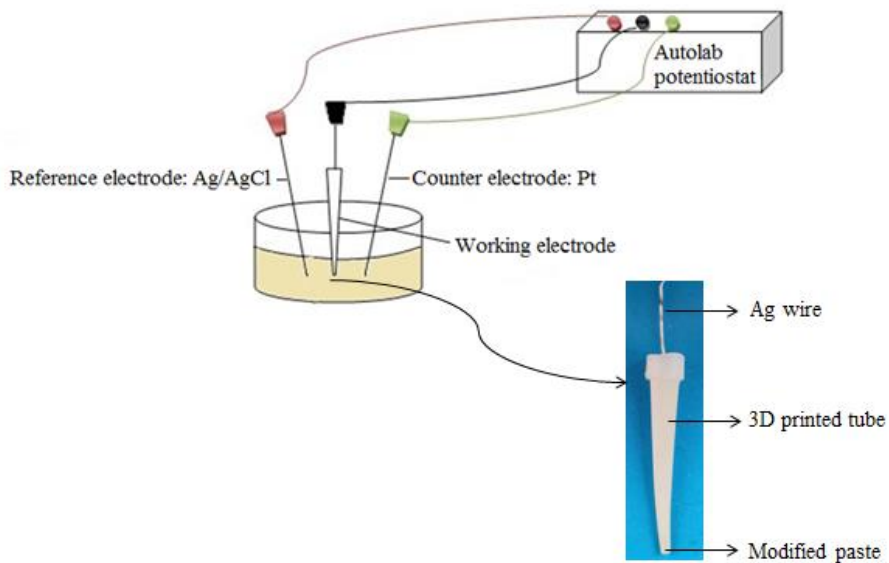
Figure 3.1. Schematic design of the 3D printed stochastic sensor and the working cell

a)

b)
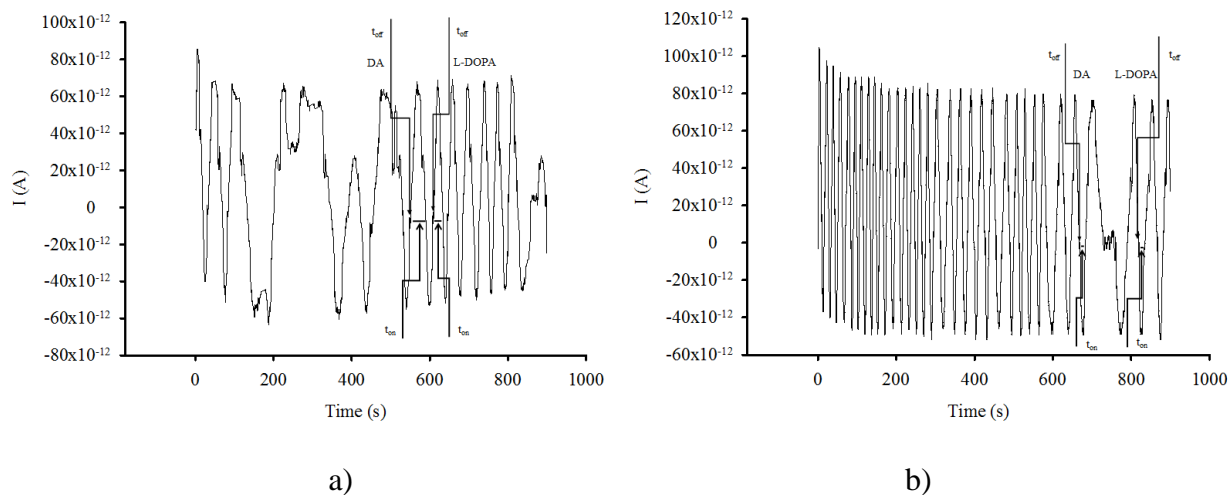
Figure 3.2. Pattern recognition of levodopa and dopamine in whole blood samples using

the stochastic sensors based on (a) AuNTs/MWNTs and (b) 1-

adamantyloleamide/AuNTs/MWNTs
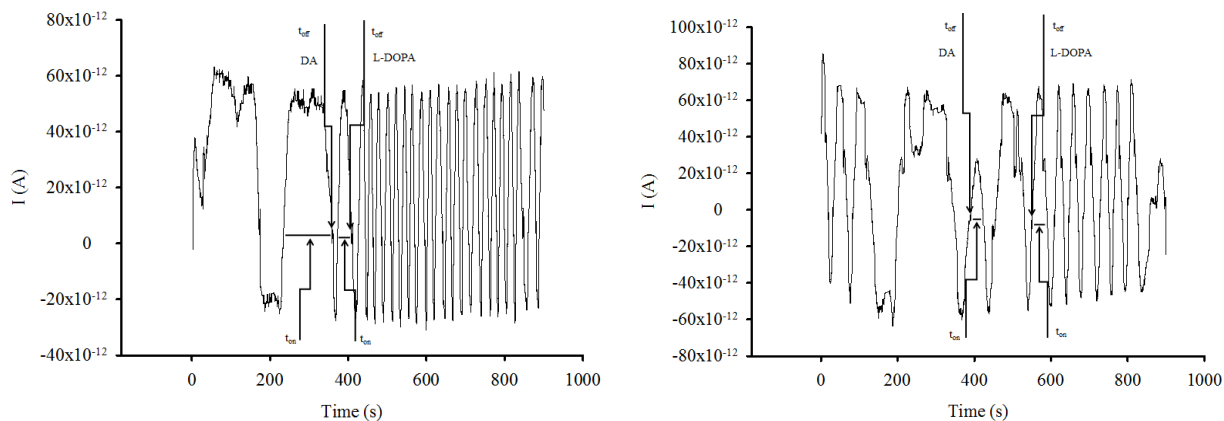
Figure 3.3. Pattern recognition of levodopa and dopamine in urine samples using the stochastic sensors based on (a) AuNTs/MWNTs and (b) 1-adamantyloleamide/AuNTs/MWNTs
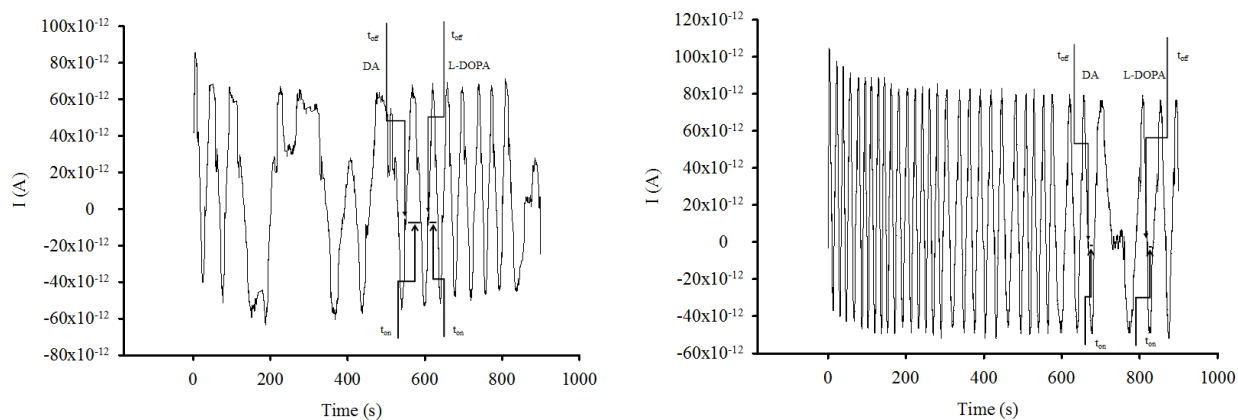
Figure 3.4. Pattern recognition of levodopa and dopamine in tumoral tissue samples using the stochastic sensors based on (a) AuNTs/MWNTs and (b) 1-adamantyloleamide/AuNTs/MWNTs

3.2.4. Samples

To validate the method, the following biological samples were analyzed: whole blood, tumor tissue and urine. Whole blood, urine, and tissue samples were collected in accordance with the procedures specified in the Ethics committee approval number 65573/14.12.2018 awarded by the University Emergency Hospital from Bucharest, from confirmed patients with brain tumor.

Written consent was obtained from all patients. After the samples were collected, immediate analysis was performed. No samples pre-treatment was performed.

3.3. Results and discussions

3.3.1. Response characteristics of the 3D stochastic microsensors

The molecular recognition of L-DOPA and DA is taking place in two steps[49,50]: the pattern recognition step when the two biomarkers are entering the channel, the intensity of the current became 0A until L-DOPA, respectively DA are inside the channel – the time needed for this step is called signature and is given by the t_{off} value. The t_{on} value is recorded during the second step characterized by binding and redox processes taken place inside the channel, therefore the t_{on} value is the quantitative parameter (Scheme 3.1).

Response characteristics of the proposed 3D stochastic microsensors were determined at two pH values: 3.00, and 7.40, to be able to cover the following types of samples: urine (with the calibration performed at pH 3.00), and whole blood and tumor tissue samples (with the calibration performed at pH 7.40). The simultaneous response characteristics for L-DOPA and DA were determined using the t_{on} values; these values are shown in Table 3. The signatures of L-DOPA and DA (t_{off} values) were different for the same 3D stochastic microsensor, indicating that the microsensors is able to perform molecular recognition of L-DOPA and DA, being selective. Accordingly, the proposed stochastic microsensors can be used for the screening tests of whole blood, urine and tissue samples.

Table 3.3. The response characteristics of the 3D stochastic microsensors used for the assay of L-DOPA and DA.

3D stochastic microsensor based on	Signature of the analyte t_{off} (s)	Linear concentration range (mol/L)	Equation of calibration; correlation coefficient, r*	Sensitivity (s mol L^{-1})	LOQ (mol/L)
AuNPs/MWNTs	L-DOPA pH=3.00				
	0.5	10^{-14}-10^{-4}	$1/t_{on}= 0.05+5.02 \times 10^{10} \times C$; r=0.9999	5.02×10^{10}	1×10^{-14}
	L-DOPA pH=7.40				
	0.7	10^{-15}-10^{-5}	$1/t_{on}=0.01+8.37 \times 10^{10} \times C$; r=0.9999	8.37×10^{10}	1×10^{-15}
	DA pH=3.00				
	1.0	10^{-14}-10^{-7}	$1/t_{on}= 0.03+2.81 \times 10^{10} \times C$; r=0.9988	2.81×10^{10}	1×10^{-14}
	DA pH=7.40				

	1.5	10^{-15}-10^{-6}	$1/t_{on}= 0.04+4.20 \times 10^{11} \times C$; r=0.9999	4.20×10^{11}	1×10^{-15}
1-adamantyloleamide/ AuNPs/MWNTs			L-DOPA pH=3.00		
	0.5	10^{-15}-10^{-3}	$1/t_{on}=0.02+4.13 \times 10^{11} \times C$; r=0.9999	4.13×10^{11}	1×10^{-15}
			L-DOPA pH=7.40		
	0.7	10^{-15}-10^{-7}	$1/t_{on}= 0.02+9.72 \times 10^{11} \times C$; r=0.9999	9.72×10^{11}	1×10^{-15}
			DA pH=3.00		
	1.0	10^{-15}-10^{-9}	$1/t_{on}= 0.04+2.19 \times 10^{12} \times C$; r=0.9999	2.19×10^{12}	1×10^{-15}
			DA pH=7.40		
	1.3	10^{-15}-10^{-7}	$1/t_{on}= 0.01+3.13 \times 10^{11} \times C$; r=0.9998	3.13×10^{11}	1×10^{-15}

*<C> =mol L^{-1}; <ton> =s; LOQ=limit of quantification.

The results from Table 3.3 shown that the addition of 1-adamantyloleamide to the paste of AuNPs/MWNTs increased the sensitivity of assay of L-DOPA and DA at pH 3.0. For pH 7.4 when DA was assayed, the sensitivity remain almost the same after the addition of 1-adamantyloleamide to the paste of AuNPs/MWNTs, while for the assay of L-DOPA, the sensitivity increased significatively when the microsensor based on 1-adamantyloleamide/AuNPs/MWNTs was used.

The limits of quantification were decreasing to 1×10^{-15} mol L^{-1} when the 1-adamantyloleamide/ AuNPs/MWNTs based microsensor was used only when the assay of L-DOPA and DA were done at pH 3.00.

Accordingly, better response characteristics were obtained by modifying the AuNPs/MWNTs paste with 1-adamantyloleamide.

The selectivity of the proposed sensors was studied also versus other neurotransmitters such as epinephrine, norepinephrine, serotonine, glutamate. The signatures (t_{off} values) of these neurotransmitters were determined using the proposed sensors, these being a measure of the selectivity of the sensors for the qualitative analysis (Table 3.4). Different values were recorded for these neurotransmitters vs L-DOPA and DA, proving that the proposed 3D stochastic microsensors are selective versus other neurotransmitters.

3D Stochastic Microsensor Based on	Signature, t_{off} (s)					
	L-DOPA	DA	Epinephrine	Norepinephrine	Serotonine	Glutamate
pH=3.0						
AuNPs/MWNTs	0.5	1.0	1.8	2.5	3.0	1.4

1-adamantyloleamide/ AuNPs/MWNTs	0.5	1.0	1.5	2.7	3.5	1.7
pH=7.4						
AuNPs/MWNTs	0.7	1.5	2.0	2.7	3.2	0.3
1-adamantyloleamide/ AuNPs/MWNTs	0.7	1.3	1.8	2.4	3.3	0.4

Table 3.4. Selectivity of the 3D printed stochastic microsensors

To prove the reliability of the design for 3D stochastic microsensors, 10 microsensors of each type were designed, and tested. The sensitivity variation was 0.12% for the microsensor based on AuNPs/MWNTs, and 0.08% for the microsensor based on 1-adamantyloleamide/ AuNPs/MWNTs. These measurements proved that the designs are reliable. The measurements were performed every day for one month, and the sensitivity was measured; in time, the sensitivity of the 3D stochastic microsensor based on AuNPs/MWNTs varied with 0.32%, while the sensitivity of the 3D stochastic microsensor based on 1-adamantyloleamide/ AuNPs/MWNTs varied with 0.21%, proving the stability of the proposed 3D microsensors in time.

Compared with the methods proposed for the simultaneous assay of L-DOPA and DA by Atta et al. [185,186] (using graphite paste modified with $SrPdO_3$ and using Nafion, carbon paste, and gold nanoparticles) the proposed method is able to perform simultaneously reliable molecular recognition of L-DOPA and DA (due to its capability of performing reliable qualitative analysis); the limits of quantification are lower than those obtained by Atta et al. [185,186], and the linear concentration ranges are far larger than those obtained by Atta et al. [185,186]. The analysis time is short: L-DOPA and DA can be determined in 6 minutes.

Compared with the methods shown in Tables 3.1 and 3.2 proposed for the assay of L-DOPA and DA, the limits of quantification are far lower, and the linear concentration ranges are wider. Also, a higher sensitivity was recorded when the 3D stochastic microsensors were used for the screening of biological samples.

3.4.Analytical applications

To demonstrate the feasibility of the proposed 3D stochastic microsensors for molecular recognition and determinations of L-DOPA and DA in whole blood and urine were performed by

spiking diluted samples with known amounts of L-DOPA and DA simultaneously. The results for the determination of L-DOPA and DA in real sample are summarized in Tables 3.5, 3.6 și 3.7. The initial values of L-DOPA and DA were determined in whole blood and urine samples. Known amounts of L-DOPA and DA were added to the samples, and the final amounts of L-DOPA and DA were determined. The recovered amount was determined by substracting from the final amount of L-DOPA and DA the amounts determined initially in whole blood and urine samples. For the 3D stochastic microsensor based on AuNPs/MWNTs, the average recovery of L-DOPA in whole blood was 93.43% with a RSD value of 1.85%, while in urine was 93.87% with a RSD value of 3.19%; the average recovery of DA in whole blood was 93.23% with a RSD value of 1.96%, while in urine was 94.62% with a RSD value of 2.68%.

For the 3D stochastic microsensor based on 1-adamantyloleamide/AuNPs/MWNTs, the average recovery of L-DOPA in whole blood was 96.00% with a RSD value of 2.35%, while in urine was 97.57% with a RSD value of 2.43%; the average recovery of DA in whole blood was 95.13% with a RSD value of 2.43%, while in urine was 96.84% with a RSD value of 4.59%.

The high values recorded for the recovery of L-DOPA and DA in whole blood and urine, as well as the good correlation between the results obtained for the recovery of L-DOPA and DA using the stochastic method and the standard method (HPLC) proved that the proposed 3D microsensors can be used for the molecular recognition and simultaneous determination of L-DOPA and DA in whole blood, urine, and tumoral tissue. Also they may be of great use for utilization in clinical studies, to determine the optimum ratio between the L-DOPA and DA, when a treatment is performed.
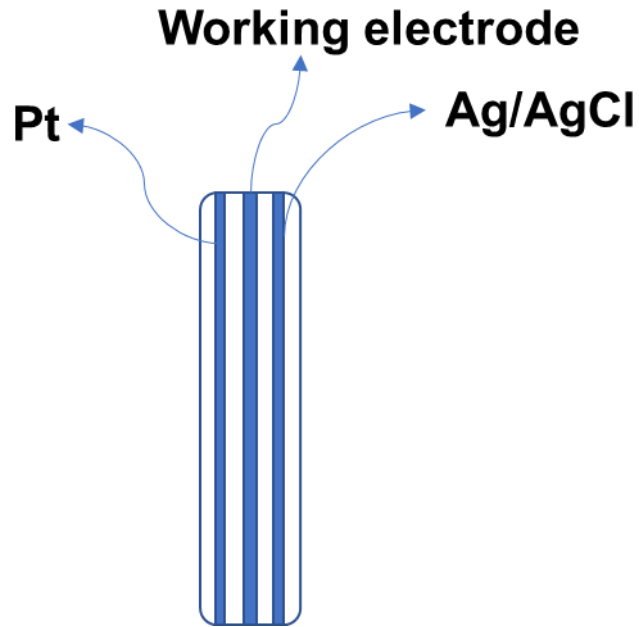
Scheme 4.1. The design of the electrochemical cell.

4.2.3. Design of the disposable stochastic sensor

Thermionic vacuum arc method, a cold plasma system, was used for the application onto commercially available silk textile of Silver nanofilm nanocoatings. The experimental setup of the plasma source was displayed in Figure 4.1.
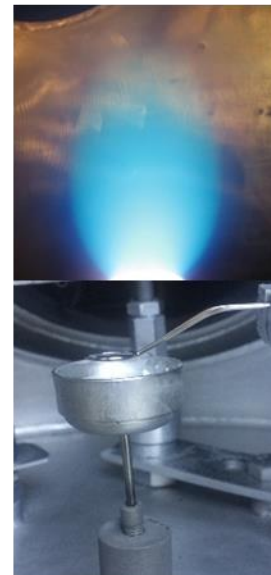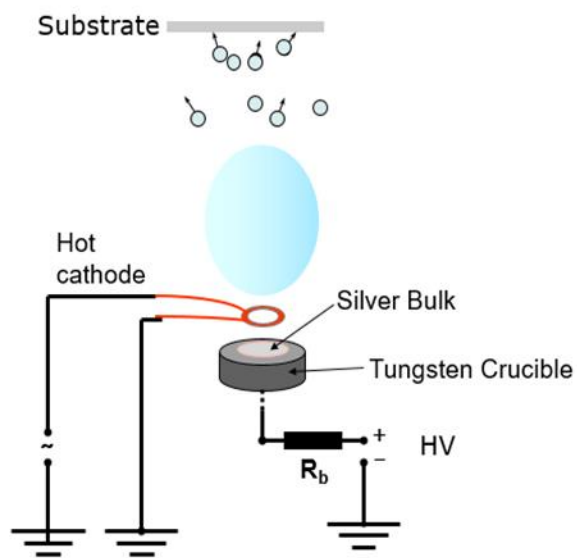
Figure 4.1. Schematic draw and real image of the cold plasma system and silver plasma plume

The ignition principle of this plasma source was based on obtaining silver vapors and ionizing them using accelerated electrons emitted from a hot cathode. The electrons were progressively accelerated by increasing the voltage at the anode (tungsten crucible) containing the silver bulk material (99.9% purity), up to a point where a stable silver plasma was obtained. The method seems to be suitable for deposition these coatings onto temperatures sensitive organic substrates materials. This method made possible to produce nanoarchitectured films coatings at very low temperature (room temperature), under high vacuum of about 10^{-6} Torr, high degree of uniformity and no buffer gas was needed.

A piece of synthetic silk with the size of 210 x 297mm was used as substrate. Before the deposition, the textile substrate was washed with deionized water and dried under nitrogen flow followed by thermal treatment in vacuum chamber for 2h to increase the surface functionalities.

For Ag deposition, the silk textile substrate was introduced in the deposition chamber which was later pumped down to ~3.0 x 10^{-6} mBar by a turbo-molecular pump. The electrical parameters used for the silver plasma were: 54A filament current, 1.6A plasma current and 250V plasma voltage. The silk substrate was placed face down at 27cm distance from the plasma plume to obtain the optimum plasma coatings. The film thickness was controlled by the deposition time and it lasted for 7 minutes. Digital photos of coated and uncoated silver nanofilm onto synthetic silk were shown in Figure 4.2.
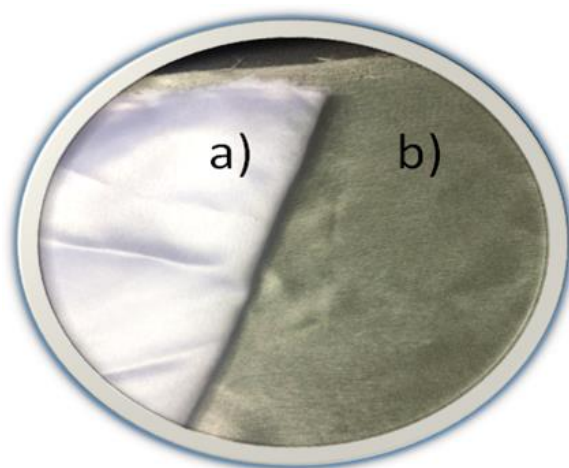
Figure 4.2. Photographs of (a) uncoated synthetic and (b) silver nanofilm coated onto synthetic silk

Synthetic silk used as a substrate for Ag nanofilm coatings in this study is illustrated by optical microscope images with different magnifications, showing differences in surface texture (Figure 4.3). Scanning electron microscopy was performed in order to characterize the surface morphologies of uncoated and coated synthetic silk.
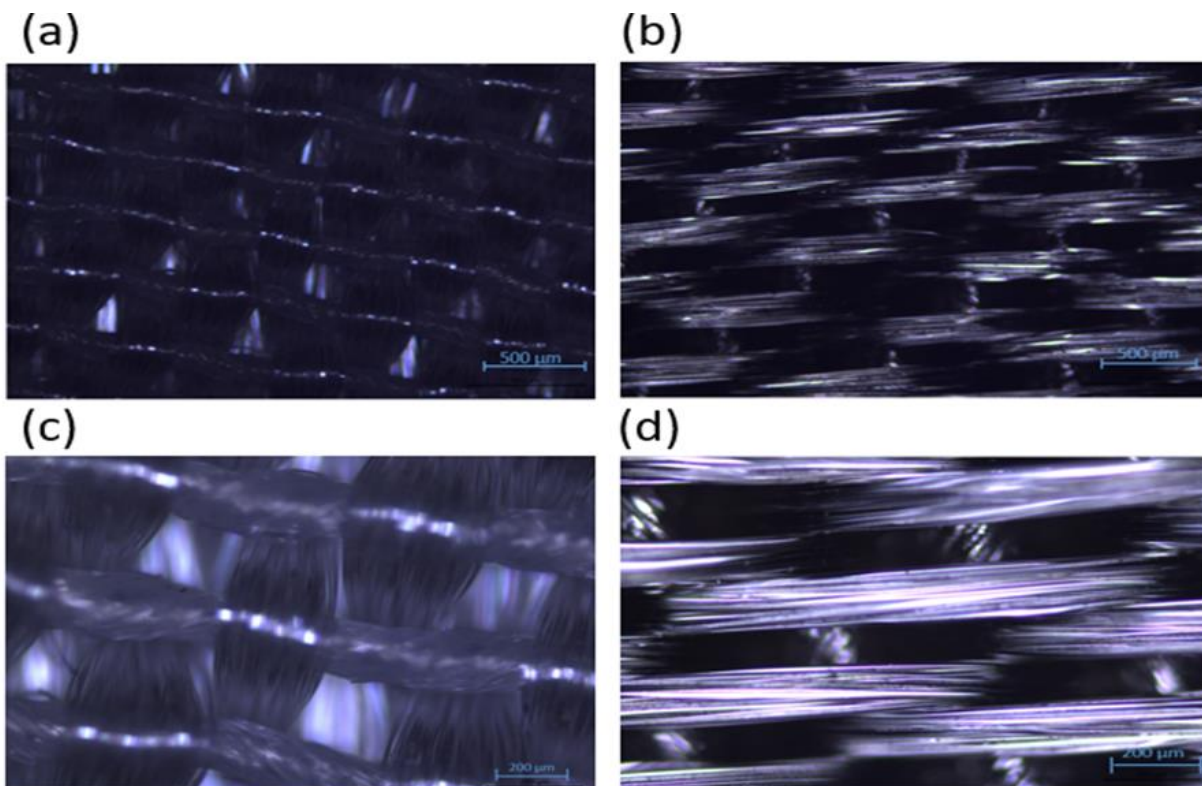
Figure 4.3. Optical microscope view of uncoated (a & c) and silver nanofilm coated (b & d) of synthetic silk; scale bar 500 µm, and 200 µm, respectively

SEM images of 250x and 63x magnification of uncoated synthetic silk are shown in Figusre 4a and 4b while in Figures 4c and 4d, 500x and 56x magnification SEM images of silver coated synthetic silk were presented. The images shown that the synthetic silk uncoated was smooth, clean, and silver nanofilm coated surface displaied a uniform and smooth coverage.
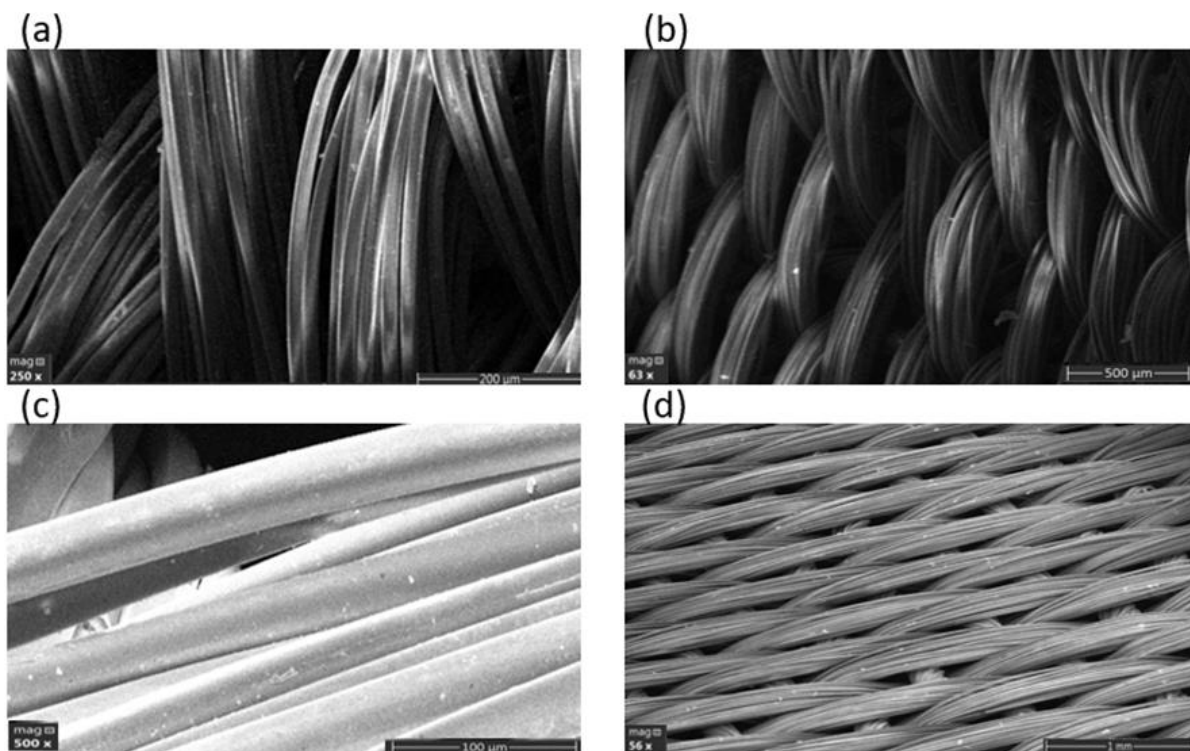
Figure 4.4 Scanning electron microscope images of synthetic silk at 4 magnifications: (a):250 x & (b): x 63k of uncoated and (c): 500 x & (d): 16x of silver nanofilm coated. The cross-sectional SEM

On the same piece of silk, left and right were deposited nanolayers of Ag/AgCl (to serve as reference electrode in the cell), and of Platinum (to serve as auxilliary electrode) (Scheme 1). The silk coated with Silver nanofilm part was soaked in a solution of 10^{-3}mol/L α-cyclodextrin for 1 h. After 1h, the silk was dried at room temperature. The width of the working electrode was 1mm. By its shape, the α-cyclodextrin can ensure the necessary channels for stochastic sensing.

4.2.4. Stochastic mode

The stochastic mode is based on the channel conductivity. The signatures of the three analites (t_{off} values) were used for their molecular recognition (by identification of their signatures in the diagrams, Scheme 4.2, Figure 4.5),) while the t_{on} corresponding values found in the diagrams recorded for the biological samples (Figure 4.5) were used for the quantitative determination of the analites accordingly with the equation: [187-190]

$$1/t_{on} = a + b \times Conc._{analyte}$$
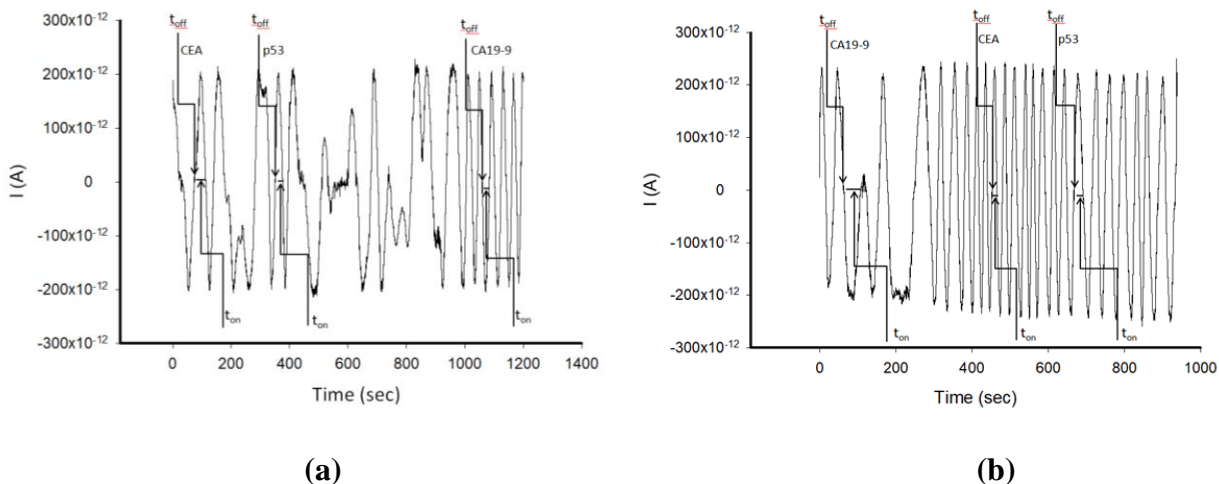
Figure 4.5. Diagrams recorded for the molecular recognition of carbohydrate antigen 19-9, carcinoembryonic antigen and serum protein p53 using the proposed disposable sensor in a) whole blood samples and b) tissue samples

All measurements were done using the chronoamperometric technique, at 125 mV vs Ag/AgCl, at 25 °C. The equations of calibrations were obtained, after screening for each biomarker solutions containing different concentrations of biomarker; linear regression method was used for determination of the equation of calibration.

4.2.5. Biological samples

Whole blood and tissue samples (Ethics committee approval number 65573/14.12.2018 awarded by the University Emergency Hospital from Bucharest) were collected from patients with confirmed glioblastoma. The samples were analyzed as collected from patients, without any pretreatment. Informed consent was obtained from all patients.

A drop of whole blood samples was placed on the disposable sensor and measured; the tissue sample was placed on top of the disposable sensor, and measured.

4.2.6. Results and discussions

The response of the disposable stochastic sensors was based on channel conductivity [187-190]. The sensing mechanism takes place in two steps:

(1) **molecular recognition step** (qualitative analysis takes place) - since entering the channel, the analyte blocks the channel and the current drops to zero for a certain time (until the

entire molecule enter the channel) called the signature of the analyte (found in the diagrams as t_{off}); (2) **analysis step** (quantitative analysis takes place) - the analyte binds the internal channel wall and undergo redox process for a certain time– found in the diagrams as t_{on}, which is correlated with the concentration of the analyte (Scheme 4.1, Figure 4.5). The biomarkers are going one by one in the channel (Scheme 4.2, Figure 4.5).
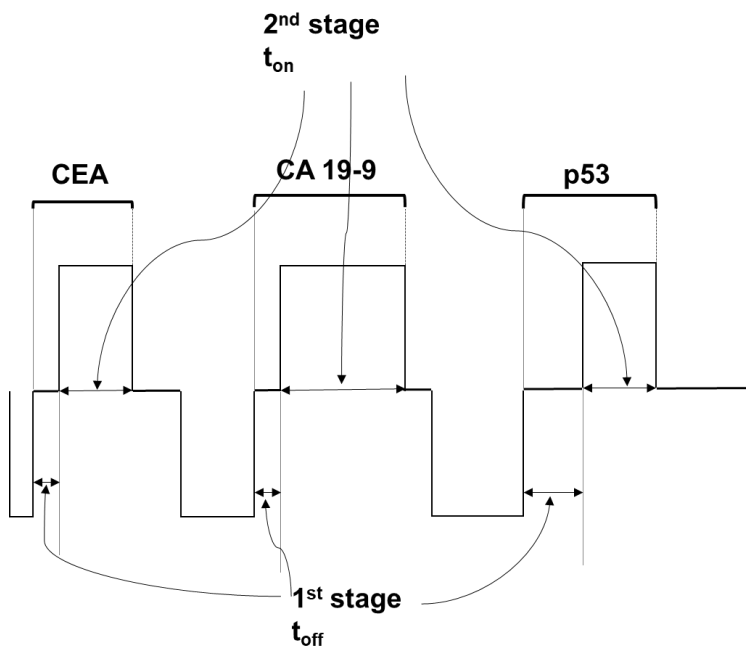
Scheme 4.2. Sensing mechanism of disposable stochastic sensor

Table 4.1. Response characteristics of the disposable stochastic sensors used for the assay of CA19-9, CEA and p53

Biomarker	Calibration equation and correlation coefficient (r)	Linear concentration range	t_{off} (s)	Sensitivity (s^{-1}/Conc. units)	Limit of determination
CA19-9*	$1/t_{on}=0.035+6.28 \times 10^9 \times C$ r=0.9991	2.1×10^{-13} – 200	0.5	6.28×10^9	2.1×10^{-13}
CEA**	$1/t_{on}=0.028+1.52 \times 10^5 \times C$ r=0.9992	4.09×10^{-9} – 3.20×10^{-4}	2.0	1.52×10^5	4.09×10^{-9}
p53**	$1/t_{on}=0.013+1.84 \times 10^2 \times C$ r=0.9897	2.56×10^{-6} – 3.2×10^{-4}	1.4	1.84×10^2	2.56×10^{-6}

Concentration units: *U/mL, **□g/mL; $<t_{on}>$=s

Different signatures (t_{off} values) recorded for the biomarkers (Tabelul 4.1) allow their simultaneous molecular recognition. The disposable stochastic sensor based on silk material gave high values of sensitivity and low limits of determination for the assay of CA19-9, CEA and p53. The linear concentration ranges covered both healthy and GBM confirmed patients. Different strips were used for measurements – the sensitivity recorded varying with less than 1.00%; this result proved the reproducibility of the design of the disposable stochastic sensor.

Comparing the proposed disposable sensor with 3D sensors based on graphene materials [192] reported previously, one should conclude that: the sensitivity of the proposed disposable sensor is higher than of those based on graphene materials; the sensor is also cost-effective – its production cost is ten times lower than the cost of any of the graphene-based 3D sensors; no contamination from previous samples can be claimed, because it is used just for measurement of one sample.

The selectivity of the sensor is given by the signatures (t_{off} values) of different biomarkers – recorded on the molecular recognition step. The signature of the analyte and possible interferent depends on many factors such as: unfolding capacity (if there are 2D/3D structures), size of the molecule, conformation of the molecule, velocity of going inside the channel; therefore, the

signature can act as molecular recognition element, contributing to qualitative analysis of mixtures. Different signatures obtained for biomarkers like CEA19-9, p53, CA19-9, KRAS, maspin, D-aspartic acid, D-glutamine proved the selectivity of the proposed disposable stochastic sensor (Table 4.2). The $t_{off\ values}$ recorded in Table 4.2 were determined in the synthetic mixture containing all biomarkers; despite the concentration of the biomarkers, the t_{off} values did not change.

Table 4.2. Selectivity of the disposable stochastic sensor (N=10)

Biomarker	Signature, t_{off} (s)
CA19-9	0.5±0.1
CEA	2.0±0.1
p53	1.4±0.2
KRAS	3.7±0.2
Maspin	1.0±0.1
D-aspartic acid	2.4±0.2
D-glutamine	3.1±0.2

4.2.7. Determination of p53, CEA and CA19-9 in whole blood and tumor tissue samples

The molecular recognition of p53, CEA, and CA19-9 was performed first using the signature of these biomarkers using the disposable stochastic sensor (Table 4.1). The t_{on} values determined from diagrams were used for the quantitative determination of these biomarkers in the biological samples, accordingly with the procedure described above in the stochastic mode. The results obtained for the assay of the three biomarkers using the disposable stochastic sensor and the results obtained using the ELISA – the standard method (Tabelul 4.3) shown a high correlation between the results obtained the proposed method and the standard method.

Table 4.3. Determination of CEA, CA 19-9 and p53 in whole blood and tumor tissue samples

Sample no.	Method	CEA (ng mL^{-1})	CA 19-9 (U mL^{-1})	p53 (ng mL^{-1})
Whole blood samples				
1	Screening method	10.29±0.21	39.43±0.21	8.32±0.27
	Standard method	9.98±1.08	39.65±2.76	8.21±1.45
2	Screening method	18.99±0.11	131.21±0.21	6.73±0.18
	Standard method	18.12±1.16	130.09±2.12	6.50±1.32
3	Screening method	90.12±0.08	183.78±0.18	8.06±0.21
	Standard method	90.98±2.12	181.97±2.21	8.95±1.07
4	Screening method	90.13±0.12	119.21±0.22	13.12±0.10
	Standard method	90.12±1.95	118.76±2.40	13.46±1.09
5	Screening method	16.09±0.18	26.65±0.11	16.70±0.14
	Standard method	15.87±1.12	26.00±1.98	16.23±1.97
Tumor tissue samples				
6	Screening method	28.14±0.21	121.55±0.11	25.82±0.23
	Standard method	27.93±1.15	120.98±1.97	25.18±1.80
7	Screening method	35.99±0.10	45.22±0.18	20.31±0.12
	Standard method	34.87±2.07	45.15±1.13	20.12±1.20
8	Screening method	15.96±0.11	112.45±0.21	45.70±0.33
	Standard method	15.15±1.23	110.95±2.21	45.32±1.23
9	Screening method	11.83±0.43	131.74±0.12	13.13±0.07
	Standard method	10.97±1.86	130.19±2.12	13.00±1.06
10	Screening method	37.50±0.18	129.29±0.40	9.31±0.10
	Standard method	37.53±1.98	128.49±1.97	9.54±1.80
11	Screening method	13.62±0.47	109.58±0.37	1.02±0.02
	Standard method	13.10±1.28	110.08±1.43	1.18±1.08
12	Screening method	67.33±0.13	173.20±0.21	47.83±0.14
	Standard method	67.62±1.97	170.94±1.15	47.20±1.21

*All values are the average of 10 determinations. Screening method was using the disposable stochastic sensor. Standard method used was ELISA.

Accordingly, the new material synthesised for the design of the disposable stochastic sensor can be reliable used for molecular recognition and also for the reliable determination of biomarkers such as CEA, p53, and CA19-9 in biological samples such as whole blood and tissue samples.

CHAPTER 5. STOCHASTIC SENSORS USED IN SIMULTANEOUS DETECTION OF IL-6, IL-12 ŞI IL 1 B

5.2.3. Design of stochastic microsensors

The nanodiamond powder was mixed with the paraffin oil in order to obtain a homogenous mixture that was further modified with a protoporphyrin IX solution (10-3 mol/L) in a ratio of 1:1 (m/v, mg/μL). The paste was introduced in a nonconducting polymer tube with an inner diameter of 10μm and the connection with the external circuit was made with a silver wire. The sensor has been cleaned with deionized water before each measurement, and kept refrigerated at 2-8 °C when not in use.

5.2.4. Stochastic mode

All measurements were performed at 25°C by using a chronoamperometric method at a constant potential of 125 mV. The signatures (t_{off} values) of the interleukins were used for qualitative analysis (identification of the interleukins on the diagrams Figure 5.1, Table 5.2). The t_{on} values were used for quantitative measurements, and were read in between two t_{off} values. The t_{on} values were determined for each concentration of interleukins, and used, using the linear regression method, for determination of the equation of calibration. For the biological samples, the t_{on} values were read in the diagrams; using the equations of calibration the unknown concentrations of the interleukins was determined.

Table 5.2. Response characteristics of the needle stochastic sensor used for the assay of IL-1β, IL-6, and IL-12.

Interleukin	Calibration equation* and correlation coefficient (r)	Linear concentration range (μg mL^{-1})	t_{off} (s)	Sensitivity (s^{-1}/g mL^{-1})	Limit of determination (μg*mL^{-1})
1β	$1/t_{on}$=0.01+4.08x10^{5}xC r=0.9999	4.0x10^{-9} – 6.4x10^{-5}	0.6±0.1	4.08x10^5	4.0x10^{-9}
6	$1/t_{on}$=0.03+1.76x10^{5}xC r=0.9999	4.0x10^{-9} – 1.0	1.8±0.2	1.76x10^5	4.0x10^{-9}
12	$1/t_{on}$=0.01+2.62x10^{3}xC r=0.9999	5.10x10^{-7} – 8.0x10^{-3}	1.3±0.1	2.62x10^3	5.10x10^{-7}

*<$1/t_{on}$> = S^{-1}, <C> = μg mL^{-1}

5.2.5. Samples

Samples (whole blood, urine, and tumor tissue) from confirmed patients with brain tumor (Ethics committee approval number 11/2013 awarded by the University Emergency , Bucharest) were analysed without any processing. Informed consent was obtained from all patients.

5.3.Results and discussions

5.3.1. Response characteristics of stochastic microsensors

The response of the needle stochastic sensor is based on channel conductivity. There are two stages: in the first stage the interleukin enters the channel, blocking it (the current drops to zero); in the second stage the interleukins undergo binding (the binding with the wall takes place) and redox process. The first stage is characterized by the signature of the interleukin (t_{off} value) and the second stage is characterized by t_{on} value (Figure 5.1).

The response characteristics were shown in Table 5.2. The signatures (t_{off} values) are different for the three interleukins proving that their simultaneous assay is possible. The linear concentration ranges recorded for each interleukin are wide, and the limits of determination made possible their assay in asymptomatic patients as well as in patients with brain cancer. The sensitivities recorded for the needle sensors are high, the highest being recorded for IL-1β and IL-6.

The stability of the needle stochastic sensor was tested every day during a period of 6 months, when the sensitivity of the senosr did not change with more than 1.00% for each of the

interleukins (0.38% for IL-1β, 0.73% for IL-6, and 0.84% for IL-12). Ten needle stochastic sensors were design accordingly with the procedure described earlier; comparing the sensitivities recorded for these sensors when used for the calibration graphs of IL-1β, IL-6, and IL-12, the relative standard deviation was less than 0.80% (0.23% for IL-1β, 0.21% for IL-6, and 0.20% for IL-12), proving the reliability of the sensor's design.

The selectivity of the needle stochastic sensor is given by the t_{off} values (signatures) recorded for the interleukins and other tumoral biomarkers such as CEA, p53, CA19-9, HER 1. According with the data shown in Table 2, the 3 interleukins had different signatures, and therefore the sensor is selective. The signatures recorded for: CEA (2.3±0.2s), p53 (4.2±0.2s), CA19-9 (2.8±0.1s), HER 1 (3.5±0.2s), dopamine (3.7±0.2s), leucine (3.1±0.1) shown that the proposed sensor is selective also versus these biomarkers.

5.3.2. Analytical applications

Tumoral tissue, urine, and whole blood samples from confirmed patients with tumor brain and healthy patients were analyzed without sample processing. The diagrams were recorded and the signatures of IL-1β, IL-6, and IL-12 identified (table 5.2); the ton values were read in between two toff (signatures), and they were introduced in the equations of calibration to find the concentrations.

Urine, and whole blood samples taken from healthy patients, and parts of brain tissue without tumor were used for recovery tests. To perform the recovery tests (the first step of validation) the original sample was analysed using the needle stochastic sensor, and after that different amounts of IL-1β, IL-6, and IL-12 were added to the samples when new analyses were performed using the needle stochastic sensor after each addition; the recovered amount of each interleukin was compared with the added amount. The results obtained were shown in Table 3. Higher recoveries than 96.00% with RSD (%) values lower than 0.07% shown the high reliability of the needle stochastic sensor for the simultaneous assay of the interleukins in biological samples.

The results obtained for the determination of the interleukins in biological samples were shown in Table 5.3. ELISA was used for the assay of the proposed interleukins – as standard method. Paired t-tests at 99.00% confidence level were performed for the assay of each interleukin, using all results shown in Table 5.3. All values calculated for the paired t test at the 99.00% confidence level were less than the tabulated theoretical value: 4.032: for IL-1β the values recorded

for whole blood, urine, and tissue analysis were 2.15, 2.93, and 3.01; for IL-6 the values recorded for whole blood, urine, and tissue analysis were 2.92, 3.13, and 2.87, and for IL-12 the values recorded for whole blood, urine, and tissue analysis were 2.14, 3.13, and 2.20. Accordingly, there is no statistically significant difference between the results obtained using the proposed needle stochastic sensor and ELISA at 99.00% confidence level, for the assay of IL-1β, IL-6, and IL-12 in biological samples. Therefore, the proposed needle stochastic sensor can be used for fast screening tests of biological fluids for the assessment of IL-1β, IL-6, and IL-12, in order to early diagnose the brain cancer.

Compared with other methods proposed to date for the determination of IL-1β, IL-6, and IL-12 [6-21], as well as with ELISA (the standard method used in the clinical labratories) the screening method using the needle stochastic sensor is more sensitive, highly reliable, cost-effective, and can be applied for simultaneous assay of the three interleukins in tissue samples, whole blood and urine without processing of these samples.

CHAPTER 6. DETECTION OF IDH-1 ȘI IDH2 FROM BLOOD OR TISSUE USING STOCHASTIC SENSORS

6.2.3. Design of 3D stochastic microsensors

100 mg SWCNT powder and MWCNT respectively, were mixed with 10 μL of gold nanoparticles dispersion which contained 1 mg powder copper, and paraffin oil until two homogeneous pastes were obtained. In order to obtain the modified pastes, 100 μL solution of PIX (1.00×10^{-3} mol L^{-1}, prepared in tetrahydrofuran) was added to each of the pastes. The morphology of the pastes that contain the necessary channels for the stochastic response are shown in Figure 6.1 (a and b). In order to evaluate the elemental composition, the quantification of the elements and their distribution in the material, a semi-quantitative analysis was performed by EDX. Also, from the mapping it may see the uniform distribution of the elements in the both modified pastes (Figure 6.1: a and b).
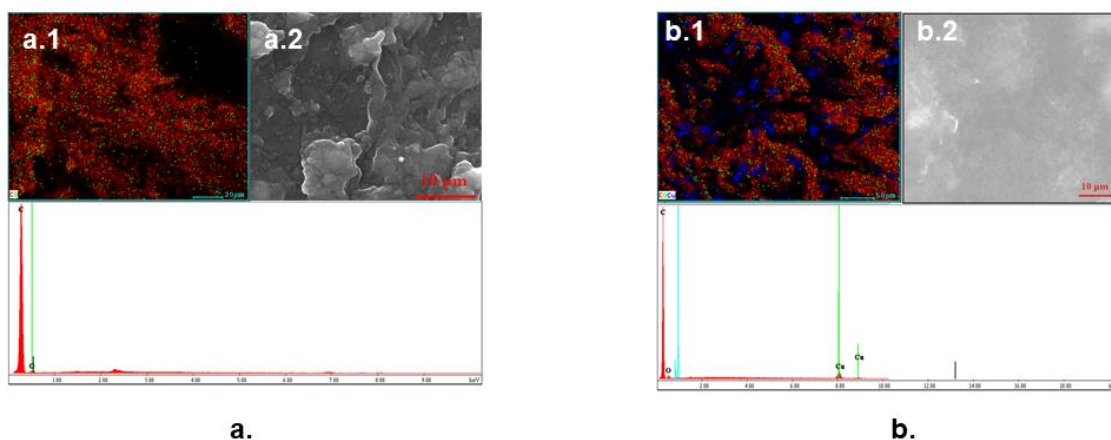
Figure 6.1. Surface analysis of the pastes based on: a. CuAuNPs-PIX/SWCNT and b.CuAuNPs-PIX/MWCNT pastes.

The modified pastes were placed in the 3D microtubes with internal diameters of 25 μm. When not in use, the stochastic microsensors were placed at 4 °C, in a dark place.

6.2.4. Stochastic mode

The chronoamperometric method was used for the qualitative and quantitative analysis of IDH1 and IDH2, based on their signatures (t_{off} values), as well as the corresponding t_{on} (which was read in between two t_{off} values) (Scheme 6.1 and Figures 6.2, 6.3). A constant potential of 125 mV *vs.* Ag/AgCl at 25°C was applied for the determination of the IDH1 and IDH2. The designed microsensors were introduced into a cell containing analyte solutions of different concentrations. The calibration equations $1/t_{on} = a + b \times C_{IDH1or2}$ were determined using the linear regression method (table 1). The concentrations of IDH1 and IDH2 in the biological samples were determined by inserting the values of $1/t_{on}$ obtained after measuring the biological samples, in the calibration equations.

The current development of stochastic sensors was shown in Scheme 6.1. Accordingly with the principles of stochastic methods, all molecules from a solution (sample) may enter into the pores/channels in function with their sizes, geometry, stereochemistry, and capacity of unfolding. As seen in the Scheme 1, the molecular recognition of the biomarkers takes place in two stages.

26

During the first stage, the analyte blocks the channel and the current intensity drops to 0 A for a period of time; this time represents the signature of the analyte (t_{off} values) and is the qualitative parameter. In the second stage, the interaction of the analyte with the wall channel, and the redox processes takes place, therefore the t_{on} value, is the quantitative parameter.
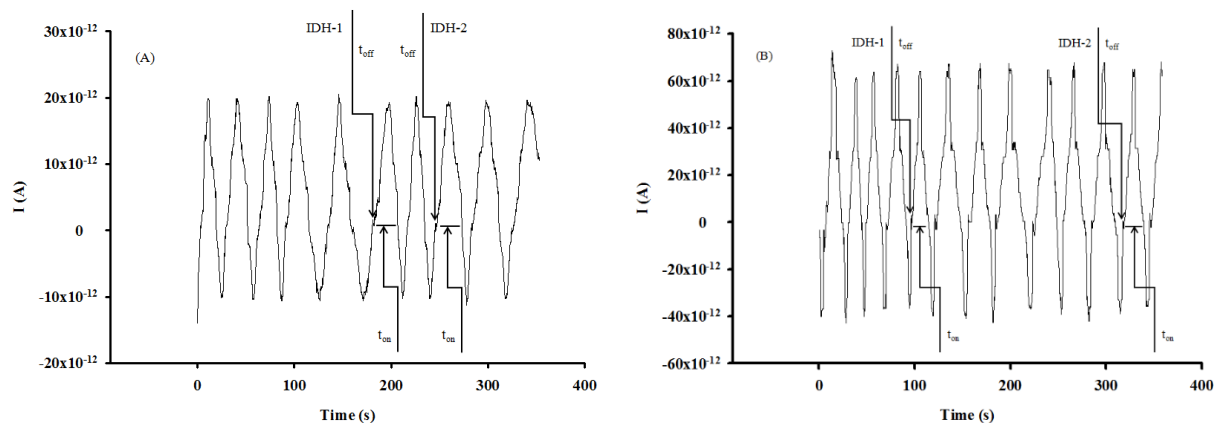
Figure 6.2. Examples of diagrams recorded for the molecular recognition of IDH1 and IDH2 in brain tumour tissue samples using the stochastic microsensors based on (A) CuAuNPs-PIX-SWCNT și (B) CuAuNPs-PIX-MWCNT
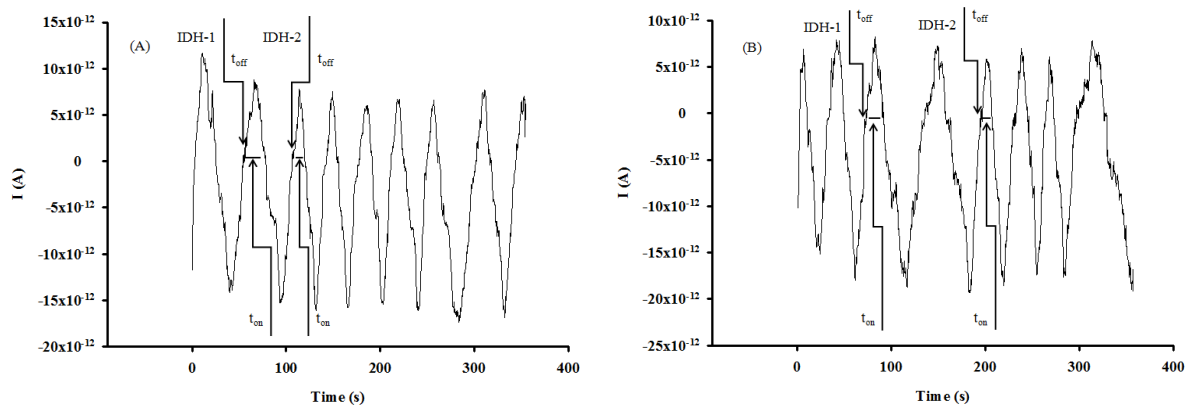
Figure 6.3. Examples of diagrams recorded for the molecular recognition of IDH1 and IDH2 in whole blood samples using the stochastic microsensors based on (A) CuAuNPs-PIX-SWCNT și (B) CuAuNPs-PIX-MWCNT

27

6.2.5. Sample preparation

The proposed 3D stochastic microsensors were used for the molecular recognition and quantitative determination of IDH1 and IDH2 in brain tumor tissue and whole blood samples. The biological samples were collected from confirmed patients with brain tumor, in accordance with the procedures specified in the Ethics Committee approval number 65573/14.12.2018 awarded by the University Emergency Hospital from Bucharest; written consent was obtained from all patients. All tissues were frozen instantly after resection and stored at temperatures of $-80°C$. The whole blood samples were used for the assay of IDH1 and IDH2 immediately after taking them from the patients, without any pre-treatment.

6.3. Results and discussions

6.3.1. Response characteristics of the stochastic microsensors

The response characteristics of the stochastic microsensors used for molecular recognition of IDH1 and IDH2 are shown in Table 1. The signatures obtained for IDH1 and IDH2 were different for each of these microsensors, thus demonstrating the ability of the microsensors to perform the molecular recognition of IDH1 and IDH2 in the biological samples.

Table 6.1. The response characteristics of the stochastic microsensors used for the molecular recognition of IDH1 and IDH2

Stochastic microsensor based on	Signature of IDH t_{off} (s)	Linear concentration range (ng mL^{-1})	Calibration equations; correlation coefficient, r*	Sensitivity (s µg mL^{-1})	LOQ (fg mL^{-1})
CuAuNPs-PIX/SWCNT	IDH1				
	0.7	$1x10^{-5}-1x10^2$	$1/t_{on}= 0.03 +1.48×C$ r=0.9999	1.48	10
	IDH2				
	1.4	$5x10^{-8}-5x10^2$	$1/t_{on}= 0.03 + 7.30×10^4×C$ r=0.9999	$7.30×10^4$	$5x10^{-3}$
CuAuNPs-PIX/MWCNT	IDH1				
	1.5	$1x10^{-5}-1x10^2$	$1/t_{on}= 0.04 + 9.58×10^5×C$ r=0.9989	$9.58×10^5$	10
	IDH2				
	0.7	$5x10^{-8}-5x10^2$	$1/t_{on}= 0.16 + 1.50×10^7×C$ r=0.9999	$1.50×10^7$	$5x10^{-3}$

*$<C>= µg$ mL^{-1}; $<t_{on}>=s$; LOQ - limit of quantification.

Utilization of SWCNT or MWCNT did not influenced the linear concentration ranges for the assay of IDH1 (1×10^{-5}-1×10^2 ng mL^{-1}) and IDH2 (5×10^{-8}- 5×10^2 ng mL^{-1}), as well as the limits of quantification for IDH1 (10 fg mL^{-1}), and IDH2 (5×10^{-3} fg mL^{-1}), but it influenced the sensitivity of the proposed stochastic microsensors – the highest sensitivity was obtained when MWCNT was used for molecular recognition of IDH1 (9.58×10^5 s µg mL^{-1}) and IDH2 (1.50×10^7 s µg mL^{-1}). Accordingly, the stochastic microsensor of choice for the molecular recognition and quantification of IDH1 and IDH2 is the one based on CuAuNPs-PIX/MWCNT.

The selectivity of the stochastic microsensors is given by the signatures (t_{off} values) recorded for different analytes. The signature of the analyte and the possible interference depends on a number of factors like: molecule size and conformation, deployment capacity, speed of going in the channel; thus, the signature can act as an element of molecular recognition, contributing to the qualitative analysis of mixtures. The different signatures obtained for analytes such as IDH1, IDH2, heregulin-α, dopamine, epinephrine, L-DOPA, proved the selectivity of the proposed stochastic microsensor (Tabelul 6.2).

Table 6.2. The selectivity of the stochastic microsensors

Stochastic microsensor based on	t_{off} (s), Signature					
	IDH1	IDH2	Heregulin-α	Dopamine	Epinephrine	L-DOPA
CuAuNPs-PIX/SWCNT	0.7	1.4	0.2	1.9	3.0	2.5
CuAuNPs-PIX/MWCNT	1.5	0.7	1.8	2.4	3.2	2.8

6.3.2. Determination of IDH1 and IDH2 in tumor bran tissue and blood samples

Eight brain tumoral tissues and 12 whole blood samples were screened using the proposed stochastic microsensors. Typical diagrams obtained for the screening tests of the brain tumoral tissue and whole blood samples (Figure 6.2 and 6.3) were used to perform the molecular recognition of IDH1 and IDH2, based on their signatures, as well as the quantification of IDH1 and IDH2 using the equations of calibration (table 1). No processing of samples was needed in the case of tissue or whole blood samples; the cell was filled with the sample, and the three electrodes inserted in the sample. After recording the diagram, the IDH1 and IDH2 were identified accordingly with their signatures, and after that the t_{on} values were determined and used in the

calibration graphs accordingly with the stochastic mode described above, for the quantification of IDH1 and IDH2.

Tables 6.3 and 6.4 shown the results obtained for the screening of tumoral brain tissues and whole blood samples. The validation of the proposed stochastic microsensors and of the screening method was done versus standard method used in the clinical laboratories for the determination – ELISA; for the assay oof IDH1, ELISA kit from Biomatik was used, while for the assay of IDH2, ELISA kit from Abbexa was used.

Paired t-test was performed at 99.00% confidence level (tabulated theoretical t-value: 4.032) for each type of sample. All calculated t-values (tables 6.3 and 6.4) were less than 3.00 proving that there is no statistically significant difference between the results obtained using the proposed stochastic sensors. Accordingly, the proposed stochastic microsensors can be reliable used for the molecular recognition and quantification of IDH1 and IDH2 in whole blood, and brain tumor tissue samples.

Table 6.3. Determination of IDH1 and IDH2 in brain tumour tissue samples using the stochastic microsensor and ELISA.

Sample no	ng mL^{-1}, IDH1		ELISA	ng mL^{-1}, IDH2		ELISA
	Stochastic microsensors based on			Stochastic microsensors based on		
	CuAuNP-PIX-SWCNT	CuAuNP-PIX-MWCNT		CuAuNP-PIX-SWCNT	CuAuNP-PIX-MWCNT	
1	15.26±0.02	16.22±0.03	16.03	26.40±0.02	26.50±0.03	26.85
2	14.03±0.03	14.52±0.02	14.48	42.42±0.03	42.65±0.04	42.82
3	14.76±0.03	16.22±0.04	16.00	27.30±0.03	28.56±0.04	27.85
4	29.97±0.03	29.62±0.02	29.03	35.60±0.04	35.27±0.03	35.57
5	9.19±0.02	9.73±0.03	9.54	63.87±0.05	64.40±0.04	63.90
6	15.26±0.03	15.02±0.04	15.05	34.77±0.03	34.68±0.02	34.70
7	6.90±0.02	6.07±0.03	6.93	22.44±0.04	21.73±0.03	22.48
8	15.85±0.03	15.14±0.02	16.12	23.02±0.02	23.72±0.05	23.80
t-test	2.94	1.83		2.87	2.08	

Table 6.4. Determination of IDH1 and IDH2 in whole blood samples using the stochastic microsensor and ELISA.

Sample no	ng mL^{-1}, IDH1		ELISA	ng mL^{-1}, IDH2		ELISA
	3D stochastic microsensors based on			3D stochastic microsensors based on		
	CuAuNP-PIX-SWCNT	CuAuNP-PIX-MWCNT		CuAuNP-PIX-SWCNT	CuAuNP-PIX-MWCNT	
1	55.25±0.03	53.56±0.02	54.24	98.64±0.02	97.98±0.02	98.70
2	77.25±0.03	73.28±0.05	75.00	70.55±0.02	71.85±0.04	70.88
3	55.24±0.04	53.35±0.05	54.28	97.30±0.03	99.00±0.08	99.02
4	10.84±0.03	9.89±0.03	10.94	34.77±0.05	34.49±0.04	35.00
5	52.75±0.03	53.66±0.05	53.84	56.68±0.03	54.52±0.04	55.94
6	5.36±0.03	5.33±0.02	5.40	21.98±0.02	22.81±0.03	23.03
7	52.97±0.03	53.34±0.04	54.02	44.14±0.02	44.95±0.05	45.00
8	13.04±0.04	13.14±0.02	13.15	20.43±0.03	20.35±0.02	21.00
9	17.50±0.03	17.69±0.04	17.70	33.38±0.04	33.61±0.05	33.54
10	14.49±0.03	13.28±0.05	14.53	35.59±0.03	34.52±0.02	35.80
11	96.48±0.01	96.34±0.02	97.00	102.36±0.03	102.65±0.02	103.00
12	14.11±0.02	14.95±0.03	15.00	26.31±0.02	26.81±0.04	26.90
t-test	2.20	1.75		2.56	2.21	

CHAPTER 7. DETECTION OF HEREGULINE α FROM BLOOD AND TISSUE

7.2. Disposable sensor used in the detection of hereguline-α

The novelty of this paper was the design of the disposable stochastic sensor: a composite material comprising graphene nanoplatelet and silver particles (GNPs-AgPs) was used for deposition of GNPs-AgPs nanofilms with cold plasma on silk. The resulting modified silk pieces were coupled with pieces covered with Ag/AgCl nanofilms (as reference electrodes), as well as with pieces covered with Pt nanofilms (as auxiliary electrode). α-Cyclodextrin was used further for modification of the GNPs-AgPs nanofilm. The resulting combined disposable stochastic sensor was used for screening tests of whole blood and brain tumor tissue samples.

7.2.1.3.Design of disposable stochastic sensors

The GNPs-AgNPs composite materials are obtained by mixing graphene nanoplates together with silver nanoparticles in a mass ratio of 2:1 with double deionized water (10 mL) to form a composite material. After that, the desired composite material was dried and heated at 100°C in a vacuum chamber, until the paste was transformed into a solid block. The coated

composite nanofilm was synthesized using a cold plasma system, thermionic vacuum arc method, onto organic based substrate such as silk textile with the size of 210×297 mm. At the outset, we implemented an external cleaning protocol for the organic based substrate, in order to remove contaminants such as particles. The deposition was carried out for 20 minutes under vacuum (1.3×10^{-5} mBar) with substrate rotation at spin speed (50 rpm) in order to form a thin film with a high uniform thickness. The electrical parameters of plasma were: 53 A filament current, 1.8 A plasma current and 200 V plasma voltage. A $1.00×10^{-3}$ mol L^{-1} solution of α-cyclodextrin was added on top of the silk pieces covered with the GNPs-AgNPs nanofilm; after two hours, they were dried for 24 h. When not in use, the disposable stochastic sensors were kept at room temperature, in a dry place. Each disposable sensor was able to be used for maximum 10 measurements. The combined disposable sensor containing also printed the Ag/AgCl (as reference electrode) and Pt (as auxilliary electrode) using the same technology is shown in Scheme 7.2.
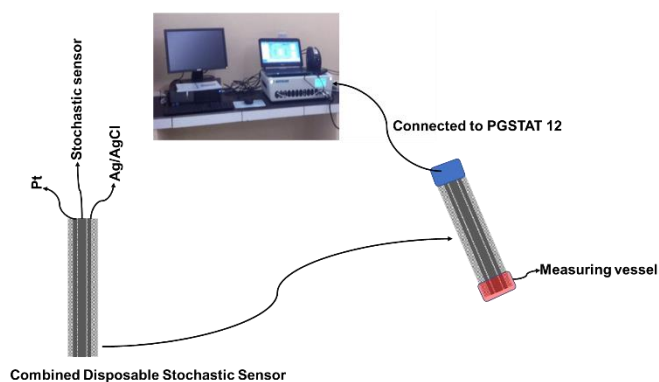
Scheme 7.2. The design of the combined disposable stochastic sensor, and its utilization for measurements.

7.2.1.4. Stochastic mode

All measurements were performed using the stochastic mode at 25°C. A potential of 125 mV *vs.* Ag/AgCl was applied. Diagrams containing t_{off} and t_{on} parameters were recorded (Figure 4). After the identification of HGR-α, by identification of its t_{off} value, the value of t_{on} was read in between two consecutive t_{off} values. The t_{on} value is connected with the concentration of HRG-α through the equation: $1/t_{on} = a + b × C_{HRG-α}$. The equation of calibration was determined using linear regression method. For the biological samples, the t_{on} values were read in the diagrams and using the equations of calibration, the unknown concentrations of HRG-α were determined.

7.2.1.5.Samples

The University Emergency Hospital from Bucharest provided the whole blood and tissue samples from patients who were diagnosed with brain cancer (informed consent was obtained from all patients, the Ethics committee of the University of Medicine and Pharmacy "Carol Davila" from Bucharest, approval number 65573/14.12.2018) in order to use them for the screening tests for HGR-α. The biological samples (1.0–2.0 mL) were used for screening tests using the proposed disposable stochastic sensor as collected from patients, without any pretreatment.

7.2.2. Results and discussions

7.2.2.1.Characterization of the material used for the design of the disposable stochastic sensor

Digital photos of coated and uncoated GNPs-AgNPs nanocomposite film one side of planar surface of a silk textile substrate are shown in Figure 1. Optical microscope images for the uncoated and coated silk textile surface are shown in Figure 2. The samples were illuminated by reflected techniques and the images are directly viewed at 5× magnification, with a resolution of 500 µm, in order to provide a good textural shape. Scanning Electron Microscopy (SEM) images of the GNPs-AgNPs nanocomposite film onto silk textile substrate are shown in Figure 3. The displayed images reveal the coated thin films uniformity on the rough surfaces with a high density of well dispersed GNPs-AgNPs composite nanofilm. Moreover, the elemental analysis of the composite nanofilms was performed by using energy-dispersive-X-ray spectroscopy (EDAX) and spectra presented in Figure 7.3 c in consistency with the proposed composition.
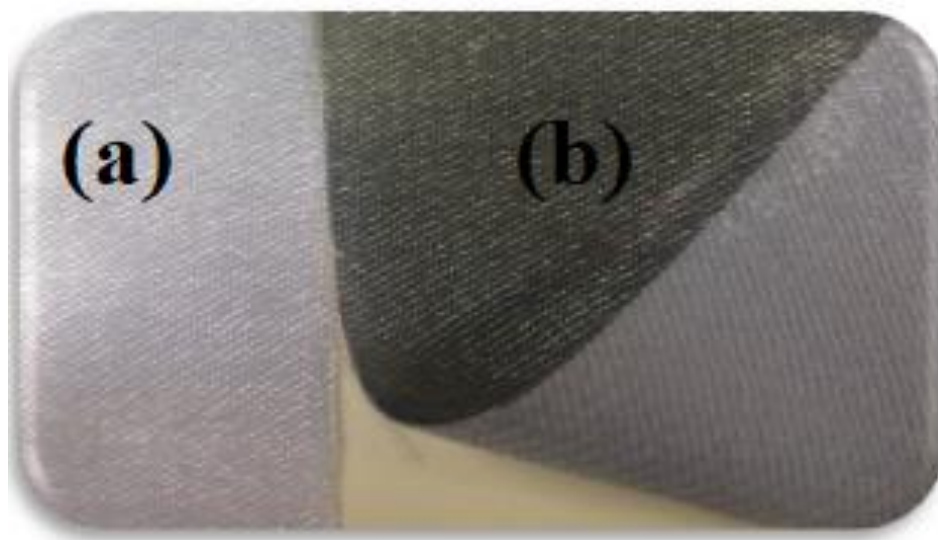
Figure 7.1. Photographs of (a) uncoated and (b) GNPs-AgNPs composite nanofilm coated onto

silk textile substrate
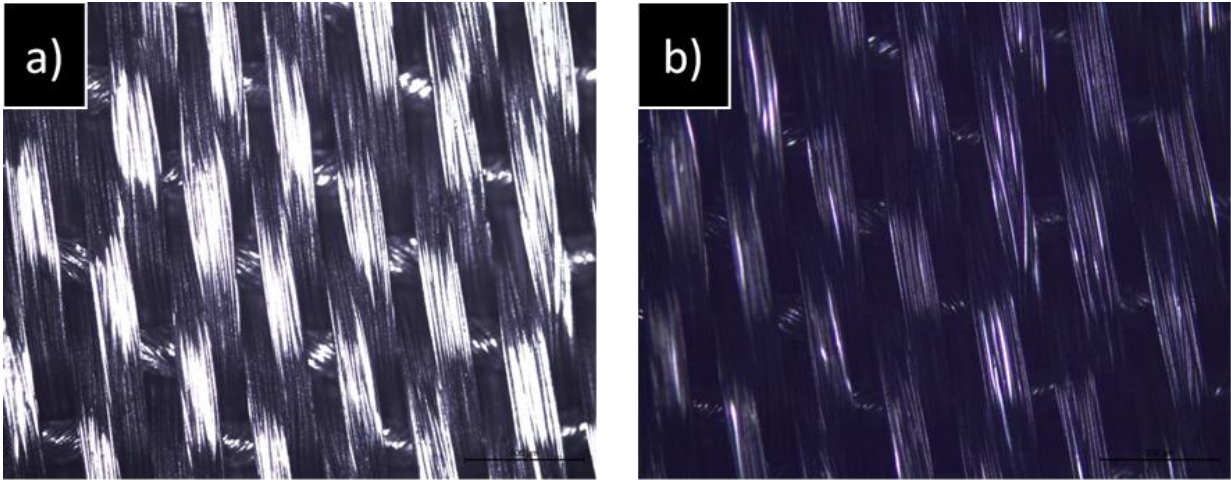
Figure 7.2. Optical microscope view of (a) uncoated and (b) GNPs-AgNPs nanocomposite film

coated onto silk textile substrate
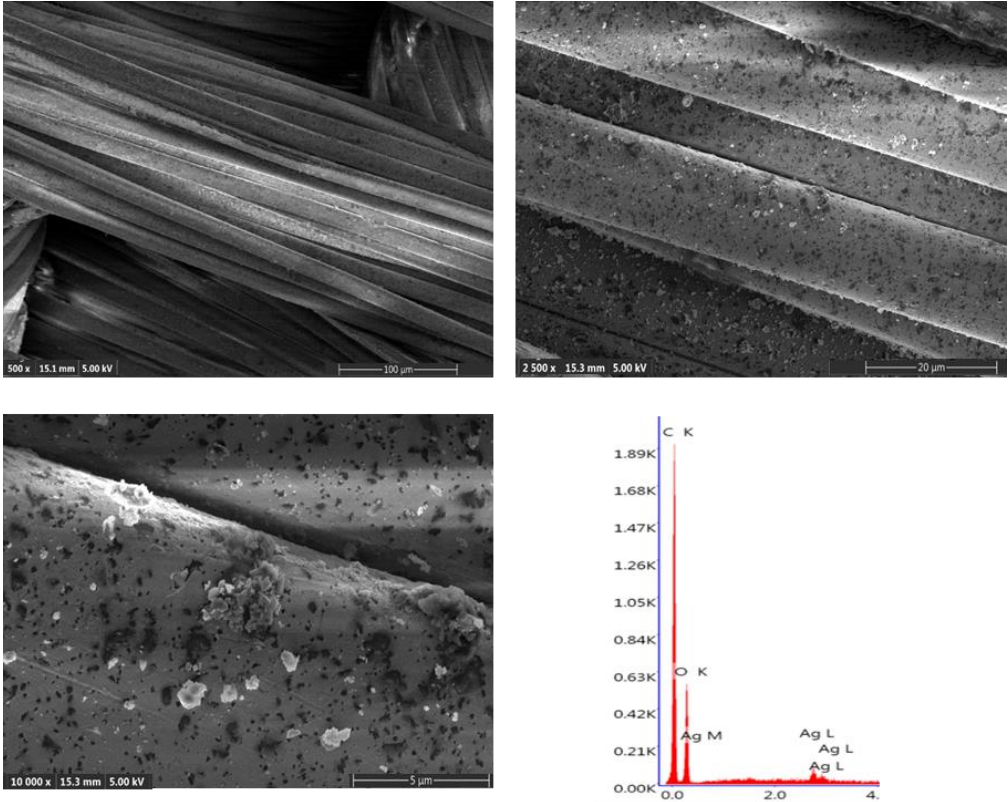
Figure 7.3. Composite nanofilms deposited onto silk textile substrate: (a-b-c) top view scanning electron microscope (SEM) image of the same sample with different magnification and (d) EDAX spectrum and elemental composition of sample

7.2.2.2.Response characteristics of the disposable stochastic sensors

The response characteristic of the disposable stochastic sensor are: the signature of HGR-α was 1.4s; the linear concentration range was between 4.10fg mL^{-1} and 0.04µg mL^{-1}, with a sensitivity of 7.21x10^{5}s µg mL^{-1}, and a limit of quantification of 4.10fg mL^{-1}. The equation of calibration was: $1/t_{on}=0.04 + 7.21x10^5C$, ($<C> = $ µg mL^{-1} and $<t_{on}> = $ s), and the correlation coefficient r of 0,9998.

The shape of the diagrams shown in Figure 7.4 examples of diagrams obtained for the screening of biological samples) shown that the binding process is reversible: alternative up and down peaks are obtained, and also there is no biofuling.

(a)   (b)
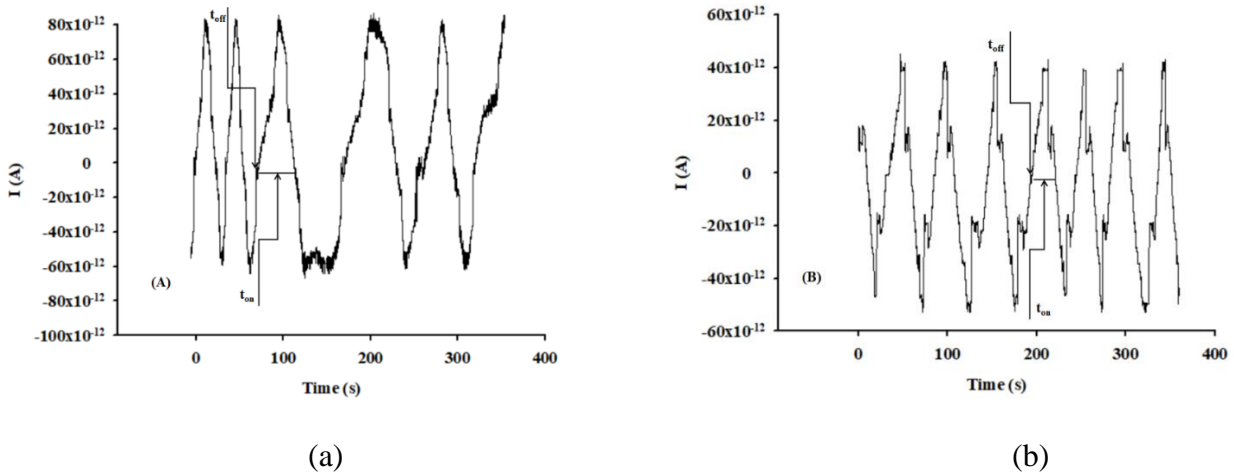
Figure 7.4. Types of diagrams recorded for the detection and quantitative determination of HRG-α in: (A) whole blood, and (B) tumoral brain tissue obtained using the screening method based on the disposable stochastic sensor

7.2.3. Selectivity of the disposable stochastic sensor

The selectivity of the proposed disposable stochastic sensor was checked versus neurotransmitters such as dopamine, epinephrine, and glutamate. The signtures (toff values recorded) of the analytes served for the determination of selectivity; the signatures obtained for dopamine (2.3s), epinephrine (1.0s), and glutamate (0.3s) are different than the one recorded for HGR-α (1.4s) proving that the proposed disposable stochastic sensors were selective versus these neurotransmitters.

7.2.4. Screening method for detection and quantification of heregulin-α in whole blood and tissue samples

The validation of the disposable stochastic sensor was done versus ELISA – the method used in clinical laboratories for the assay of HGR-α, using biological samples (whole blood, and brain tumor tissues). The results of determination of HGR-α in whole blood (Table 1) and in brain tumor tissue (Table 7.2) obtained using the screening method based on the disposable stochastic sensor as well as using the ELISA shown a very good correlation between the two methods of analysis. A paired t-test method was done for further validation of the screening method used for the detection and quantification of HRG-α. The paired t-tests were performed at 99.00% confidence level. All calculated values for the pair-t test at the 99.00% confidence level were less than the tabulated theoretical value: 4.032 (Tables 7.1 and 7.2). Accordingly, there is no statistically significant difference between the results obtained using the proposed screening method and ELISA, at 99.00% confidence level, for the assay of HRG-α in whole blood and in tumoral brain tissue. Accordingly, the screening method can be validated for the assay of HRG-α in whole blood and in tumoral brain tissue.

Table 7.1. Determination of HRG-α in whole blood samples using the disposable stochastic sensor and ELISA.

Sample No.	pg mL^{-1}, HRG-α	
	Disposable Stochastic Sensors	ELISA
1	153.60±0.18	160.03
2	486.56±0.13	430.15
3	690.50±0.13	690.12
4	999.92±0.15	993.15
5	18.66±0.11	18.50
t-test	2.08	-

Table 7.2. Determination of HRG-α in brain tumor tissue samples using the disposable stochastic sensor and ELISA.

Sample No.	pg mL^{-1}, HRG-α	
	Disposable Stochastic Sensors	ELISA
1	7.17±0.11	7.35
2	2.90±0.25	2.19
3	7.42±0.10	7.50
4	2.59±0.13	2.20
5	6.48±0.13	6.53
6	5.21±0.12	4.73
7	560.30±0.10	553.23
8	6.02±0.15	5.98
9	4.47±0.12	4.21
10	1.37±0.10	1.15
11	19.74±0.13	19.50
12	131.07±0.14	129.15
t-test	2.19	-

7.3.3D Stochastic Microsensors for Determination of Heregulin-α in Biological Samples

7.3.1. Design of 3D stochastic microsensors

21mg SWCNT powder and 25mg MWCNT powder, respectively, were mixed with paraffin oil until two homogeneous pastes were obtained. In order to obtain the modified pastes, 20μL solution of Mn(TPP)Cl (1.00×10^{-6} mol L^{-1}, in tetrahydrofuran) were added to each of the pastes. This composition was optimized until we've got the optimum stochastic signal. The morphology of the pastes was shown in Figure 1; the necessary channels needed for stochastic response are present.
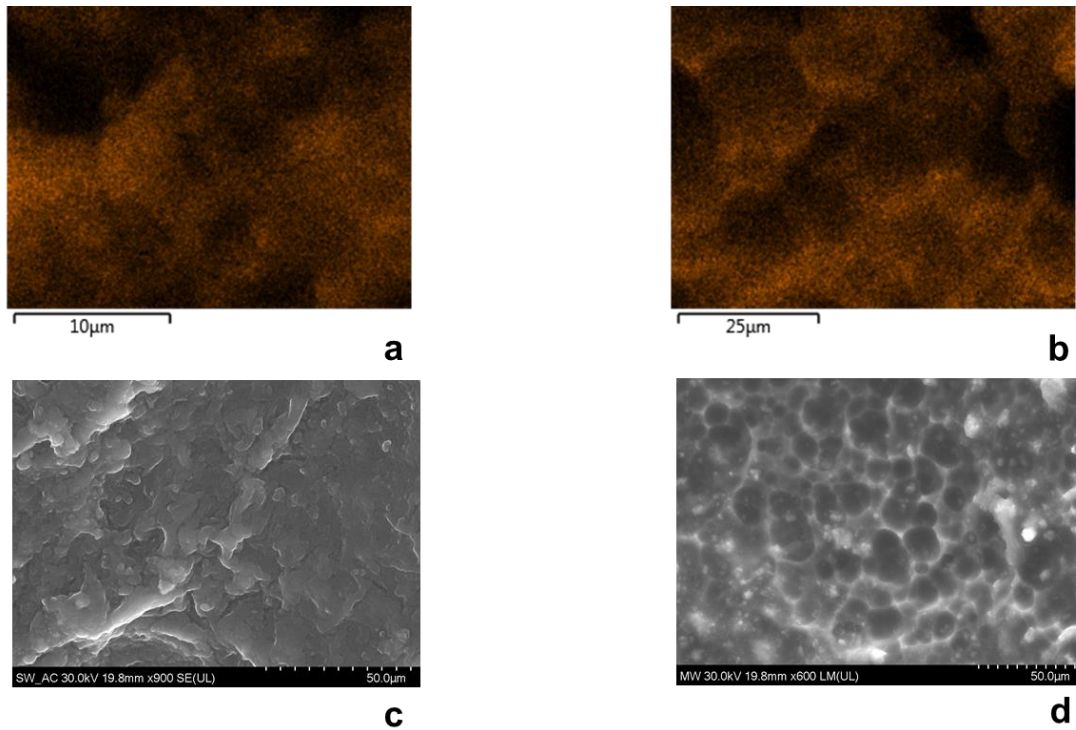
Figure 7.5. SEM images of Mn(TPP)Cl/SWCNT a) and c), and of Mn(TPP)Cl/MWCNT b) și d).

3D microtubes with internal diameters of 25µm were printed in the laboratory using a 3D printer. Each of the modified pastes was placed in the 3D printed microtubes; a silver wire served as electrical contact between the paste and external circuit. The 3D microsensors were cleaned with deionized water. When not in use, they were kept at room temperature, protected from light.

7.3.4. Stochastic mode

Solutions of heregulin-α with concentrations between 4.09fg/mL and 50µg/mL were used for finding the response characteristics including linear concentration ranges for the proposed stochastic sensors. The stochastic mode was based on current conductivity; after applying a potential of 125mV, diagrams were obtained (Figures 2 and 3), and the values of toff (the qualitative parameter used in molecular recognition) and ton (the quantitative parameter) were determined in the diagrams. First step comprising in molecular recognition of HGR-α, based on the toff value read in the diagrams. The equation of calibration $1/t_{on} = a + b \times C_{HGR-\alpha}$ was obtained using the linear regression method, and it was based on reading the ton value in between

two toff values in the diagrams. The unknown concentration of HGR-α was determined by inserting the value of 1/ton in the equation of calibration.

a)

b)
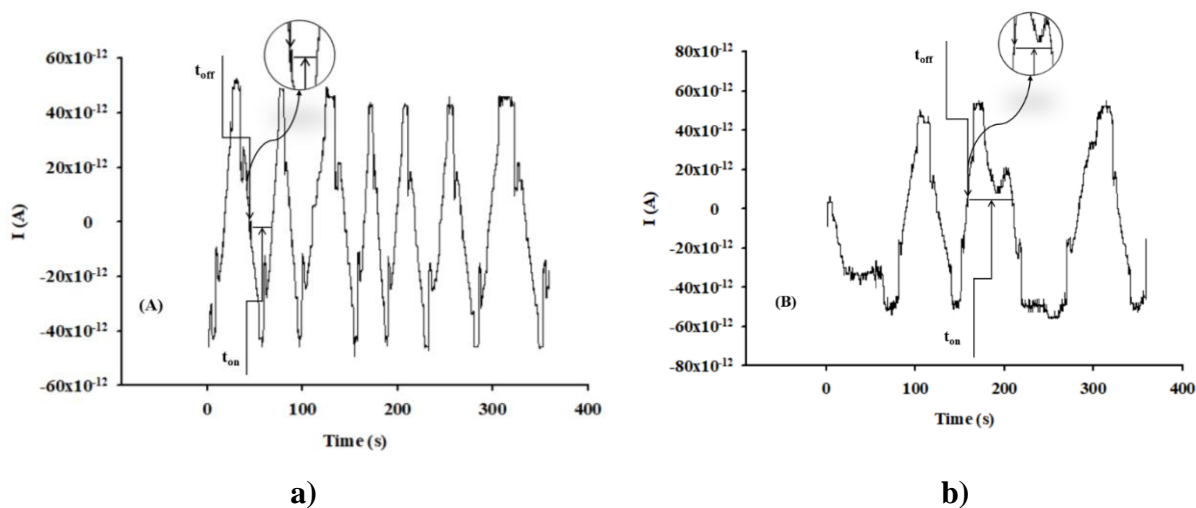
Figure 7.6. Types of diagrams recorded for the molecular recognition and quantitative determination of HRG-α in: (A) whole blood, (B) tumoral brain tissue obtained using the 3D stochastic microsensor based on Mn(TPP)Cl/SWCNT.

a)

b)
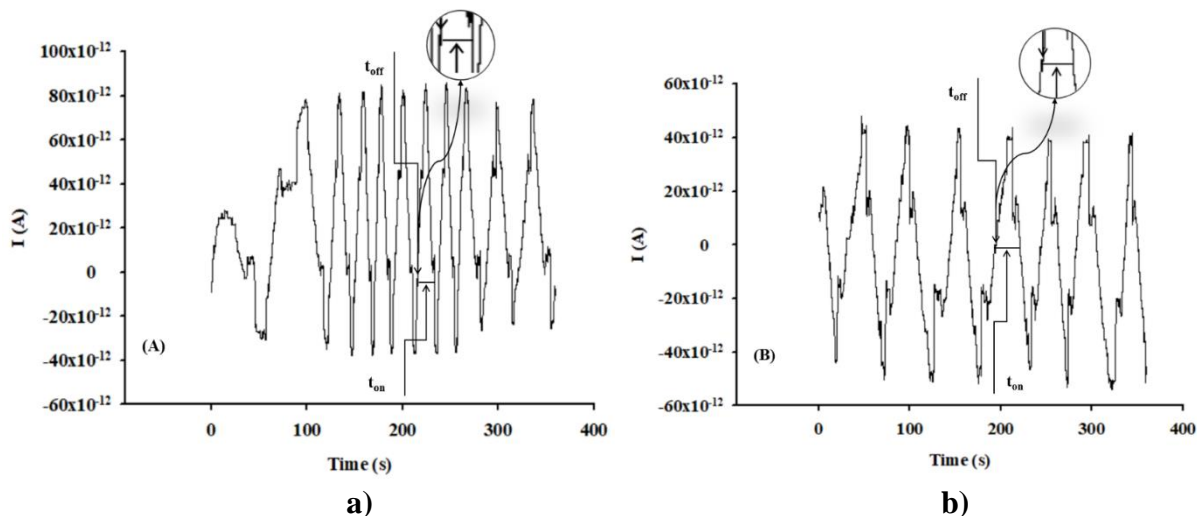
Figure 7.7. Types of diagrams recorded for the molecular recognition and quantitative determination of HRG-α in: (A) whole blood, (B) tumoral brain tissue obtained using the 3D stochastic microsensor based on Mn(TPP)Cl/MWCNT.

For the determination of heregulin-α in whole blood, the whole blood (the volume used was 300μL) was placed in the electrochemical cell, a potential of 125mV was applied for 6minutes, a diagram was obtained; the signal for heregulin-α was identified in the diagram using the t_{off} value, while the corresponding t_{on} value was read in the diagram, and used for the determination of the concentration using the equation of calibration.

The tumor tissue sample (with an area of $0.49cm^2$) was used – as taken from the patients. For the assay of heregulin-α in this samples, the three sensors: 3D stochastic microsensors, the reference, and auxilliary electrodes were placed in a miniaturized holder (Scheme 7.3), and the holder was placed on the tumor tissue as shown in Scheme 7.3.
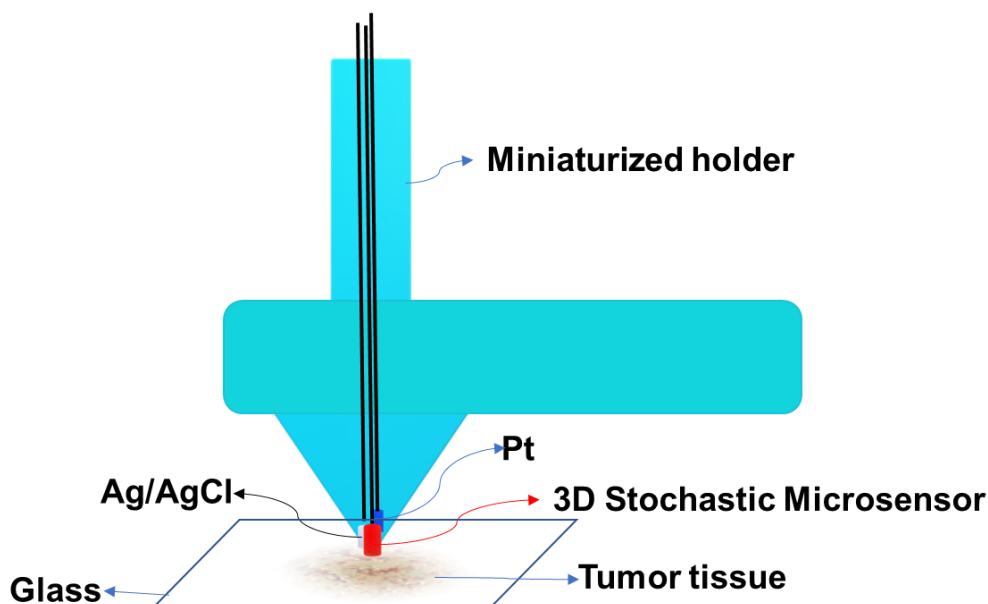
Scheme 7.3. Screening of tumour tissues with the 3D stochastic microsensor.

Measurements were performed in 10 different points on the tumor tissue. The time used for each measurement was 6minutes. On the diagrams obtained, the heregulin-α was identified

based on its t_{off} value, while the corresponding t_{on} value was used for the assay of its concentration using the equation of calibration.

7.3.5. Samples

Biological samples such as whole blood, and tumour brain tissue samples were used for the validation of the proposed 3D stochastic microsensors and the screening method used for molecular recognition and quantitative determination of HRG-α in whole blood and tumour brain tissue. The University Emergency Hospital from Bucharest provided the whole blood and tumor brain tissue samples from confirmed patients with brain cancer (informed consent was obtained from all patients, the Ethics Committee of the University of Medicine and Pharmacy "Carol Davila" from Bucharest, approval number 65573/14.12.2018). All these samples were used for the assay of HRG-α immediately after taking them from the patients, and without any pre-treatment.

7.3.6. Results and discussions

7.3.6.1. Response characteristics of the 3D stochastic microsensors

The response characteristics of the 3D stochastic microsensors based on Mn(TPP)Cl/SWCNT and on Mn(TPP)Cl/MWCNT are shown in Table 7.3.

Table 7.3. Response characteristics of the 3D stochastic microsensors.

Sensor based on	Signature of the analyte t_{off} (s)	Linear concentration range	Equation of calibration; correlation coefficient, r*	Sensitivity (s⁻¹/µg mL⁻¹)	Limit of quantification (fg mL⁻¹)
Mn(TPP)Cl/ SWCNT	2.0	102.00fg mL⁻¹ – 9.00ng mL⁻¹	$1/t_{on}=0.01 + 4.14 \times 10^4 C$; r=0.9999	4.14×10^4	102.00
Mn(TPP)Cl/ MWCNT	1.4	102.00fg mL⁻¹ – 5.00µg mL⁻¹	$1/t_{on}=0.02 + 1.36 \times 10^4 C$; r=0.9994	1.36×10^4	102.00

$*<C> = \mu g\ mL^{-1}$; $<t_{on}> = s$

First of all, the signatures of HRG-α were determined. The type of CNT influenced only the sensitivity of the 3D stochastic microsensors, although they both had sensitivities of the same magnitude order, the 3D stochastic microsensor based on Mn(TPP)Cl/SWCNT had a sensitivity more than three times higher than the 3D stochastic microsensor based on Mn(TPP)Cl/MWCNT, while the linear concentration range recorded for the 3D stochastic microsensor based on

Mn(TPP)Cl/MWCNT was far wider than the one recorded for the 3D stochastic microsensor based on Mn(TPP)Cl/SWCNT. The limits of quantification determined for both 3D stochastic microsensors had the same value: $102.00 fg\ mL^{-1}$; the type of CNT did not influence the limits of quantification. The 3D stochastic microsensor of choice is the one based on Mn(TPP)Cl/MWCNT.

Five 3D stochastic microsensors of each type were prepared and used for the assay of HRG-α; the sensitivities obtained for each microsensor were compared; for the 3D stochastic microsensor based on Mn(TPP)Cl/SWCNT, the relative standard deviation was 0.45%, while for the 3D stochastic microsensor based on Mn(TPP)Cl/MWCNT, the relative standard deviation was 0.32%. The variation of the sensitivity of each 3D stochastic microsensor was further evaluated for 1 month, when it varied with 0.09% for the 3D stochastic microsensors based on Mn(TPP)Cl/SWCNT, and with 0.12% for the 3D stochastic microsensors based on Mn(TPP)Cl/MWCNT. These measurements proved the high reliability of the design of the microsensors, and also a high stability in time of the 3D stochastic microsensors.

The selectivity was checked versus neurotransmitters such as dopamine, epinephrine, norepinephrine, and HER3. The signature of the substance determined (t_{off} value) – used in molecular recognition of the substances/biomarkers is the one giving the selectivity, in the case of stochastic sensors. Accordingly, because the signatures of dopamine, epinephrine, norepinephrine, and HER3 (table 7.4) are far different than those recorded for HRG-α, one can say that the proposed 3D stochastic microsensors are selective.

Table 7.4. The selectivity of the 3D stochastic microsensors.

Sensor based on	Signature, t_{off} (s)				
	HRG-α	Dopamine	Epinephrine	Norepinephrine	HER3
Mn(TPP)Cl/ SWCNT	2.0	0.5	1.2	2.8	3.5
Mn(TPP)Cl/ MWCNT	1.4	0.7	2.0	3.2	3.7

7.3.6.2. Analytical applications

Whole blood and brain tumoral tissue samples were used for the validation of the proposed 3D stochastic microsensors and also for the validation of the screening test method which will be used for the molecular recognition of HRG-α as well as for its quantification. The diagrams obtained in the screening tests of whole blood and brain tumoral tissue samples (Figures 7.6 and

7.7) were used to performe the molecular recognition of HRG-α, based on its signature (table 7.3). After the molecular recognition step, the t_{on} values were read (in between two consecutive t_{off} values) and used accordingly with the stochastic mode described earlier for the quantification of HRG-α.

The validation of the 3D stochastic microsensors and of the screening methods was done versus ELISA (the standard method used in the clinical laboratories for the determination of HRG-α). The results obtained for the screening of whole blood samples and of tumoral brain tissues are shown in tables 7.5 and 7.6. Very good correlations between the data obtained with the 3D stochastic microsensors and the data obtained using ELISA were recorded. t-test was also used for the validation of the microsensors and of the screening methods. The paired t-tests were permormed at 99.00% confidence level, for the results obtained using each 3D stochastic microsensors versus ELISA. All values calculated for the pair-t test at the 99.00% confidence level are less than the tabulated theoretical value: 4.032 (Tables 7.5 and 7.6 Accordingly, there is no statistically significant difference between the results obtained using the two 3D stochastic microsensors and ELISA, at 99.00% confidence level, for the assay of HRG-α in whole blood and in tumoral brain tissue. Accordingly, the two 3D stochastic microsensors and the screening methods can be validated for the assay of HRG-α in whole blood and in tumoral brain tissue.

Table 7.5. Determination of HRG-α in whole blood samples using the 3D stochastic microsensor and ELISA.

Sample No.	pg mL^{-1}, HRG-α		ELISA
	3D Stochastic Sensors Based on		
	Mn(TPP)Cl/SWCNT	Mn(TPP)Cl/MWCNT	
1	7.75±0.12	7.53±0.18	7.35
2	2.97±0.22	2.44±0.25	2.19
3	7.75±0.13	7.87±0.11	7.50
4	2.74±0.10	2.78±0.19	2.20
5	6.41±0.13	6.23±0.17	6.53
6	4.46±0.18	4.87±0.12	4.73
7	558.73±0.21	551.55±0.28	553.23
8	6.90±0.11	6.93±0.09	5.98
9	4.33±0.08	4.41±0.12	4.21
10	1.59±0.09	1.14±0.09	1.15
11	19.47±0.22	19.61±0.27	19.50
12	129.55±0.12	129.66±0.13	129.15
t-test	2.49	2.21	-

Table 7.6. Determination of HRG-α in brain tumour tissue samples using the 3D stochastic microsensor and ELISA.

Sample No.	pg mg⁻¹, HRG-α		
	3D Stochastic Sensors Based on		ELISA
	Mn(TPP)Cl/SWCNT	Mn(TPP)Cl/MWCNT	
1	157.56±0.22	158.59±0.24	160.03
2	433.09±0.32	432.65±0.25	430.15
3	697.65±0.20	695.73±0.17	690.12
4	997.65±0.35	996.30±0.32	993.15
5	18.80±0.10	18.83±0.12	18.50
t-test	2.23	2.12	-

CHAPTER 8. DETECTION OF DOPAMINE IN BLOOD USING A VOLTAMETRIC SENSOR BASED ON MODIFIEFD GRAPHENE DOPED WITH SULFUR WITH PROTOPORPHYRIN IX

8.2.3. Design of the electrochemical sensor

The graphene powder doped with sulfur was mixed with paraffin oil to obtain a homogeneous paste, which was further modified with protoporphyrin IX. A plastic tip was filled with the modified paste and the electric contact was made using a silver wire. The surface of the sensor was washed with deionized water and polished with alumina paper before each utilization. If not in use, the electrochemical sensor was kept in the fridge at 2–8°C.

8.2.4. Procedure

The differential pulse voltammetry (DPV) measurements were performed at 25°C for each standard solution (10^{-3}mol L⁻¹–10^{-12}mol L⁻¹). The working parameters were as following: scan rate was 50 mVs⁻¹, potential range 0-1000 mV, and modulation amplitude 50 mV. The peak heights intensities were measured and the equation of calibration was found using the linear regression method. The unknown concentrations were calculated from the equation of calibration determined statistically.

8.3.Results and discussion

8.3.1. Response characteristics of the graphene paste sensor

Differential pulse voltammetry (DPV) technique was used to determine the response characteristics of the electrochemical sensor. The response characteristics obtained were: the linear

concentration range was between 1.0×10^{-7} mol L^{-1} and 1.0×10^{-4} mol L^{-1}, the limit of determination was 1.0×10^{-7} mol L^{-1}, the limit of detection was 5.0×10^{-8} mol L^{-1} and the sensitivity was 1.0×10^{-3} A/mol L^{-1}. The equation for the resulting calibration plot was:

$$I = 3{,}0 \times 10^{-8} + 1{,}0 \times 10^{-4} \times C$$

where I (A) is the peak height and C is the concentration of dopamine. The correlation coefficient was 0.9994. The results showed a good value of the sensitivity and a low limit of and detection of dopamine. The linear concentration range is wide. The voltammograms used for the calibration of the proposed sensor were shown in Figure 8.1.
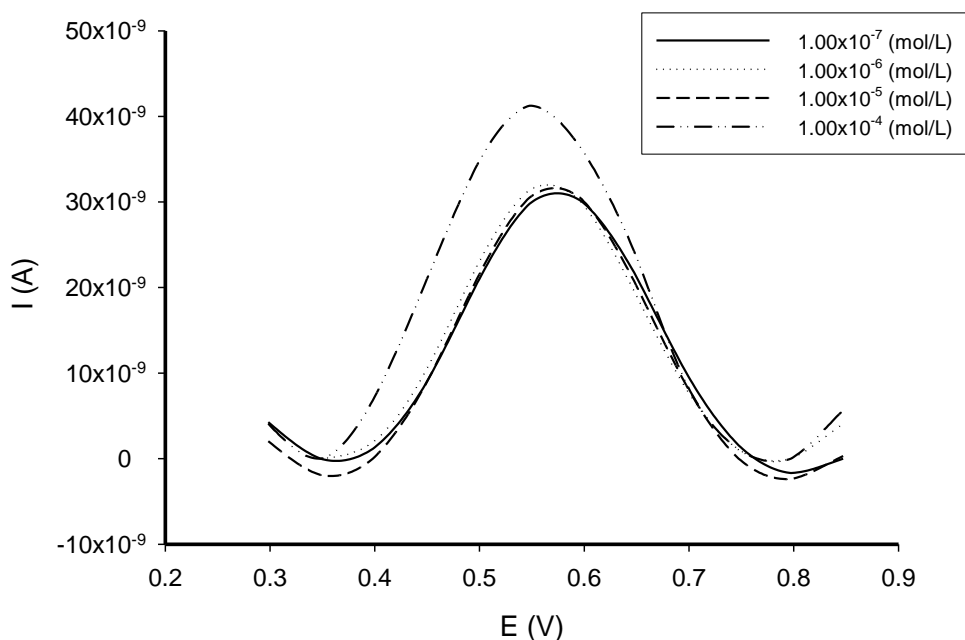
Figure 8.1. Differential pulse voltammogram obtained for dopamine at different concentrations.
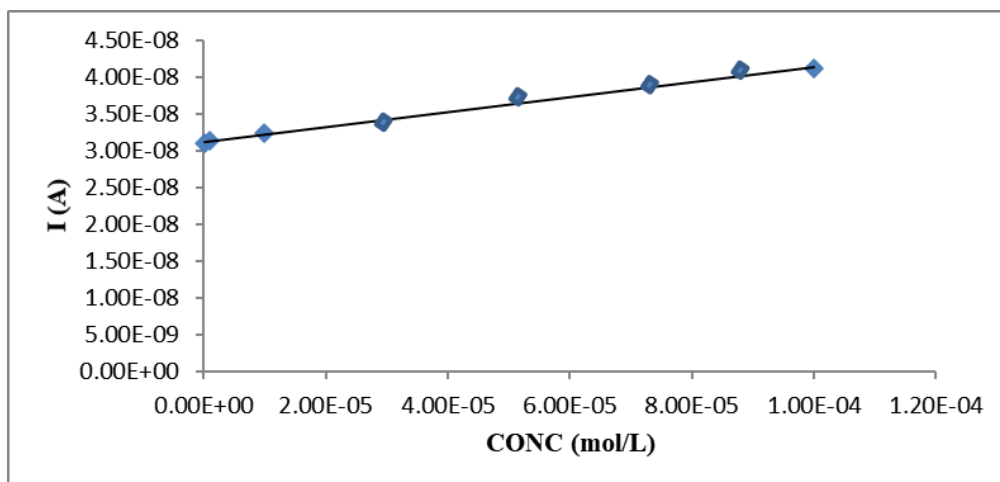
Figure 8.2. Calibration graph obtained for dopamine using the modified graphene paste based sensor.

8.3.2. *Interferences*

Ascorbic acid (AA), uric acid (UA), glutamine (GLU), L-serine (L-SER) were chosen as possible interferences for the assay of dopamine.The ratio between the concentrations of dopamine and interferent was 1:10 (mol:mol) in the mixed solution. The amperometric selectivity coefficients were determined using the following equation:

$$K_{i,j}(amp) = \left(\frac{\Delta I_t}{\Delta I_i} - 1\right) * \frac{c_i}{c_j} \qquad (16)$$

where $K_{i,j\ (amp)}$ is the amperometric selectivity coefficient, $\Delta I_t = \Delta I_t - \Delta I_b$, where ΔI_t is the total intensity of the current, ΔI_b is the intensity of the current recorded for blank solution, $\Delta I_i = \Delta I_i - \Delta I_b$, where ΔI_i is the intensity of the current registered for main ion, c_i and c_j are the concentrations of the main ion and the interfering ions.

The amperometric selectivity coefficients obtained vs AA (2.68×10^{-3}), vs UA (1.70×10^{-3}), vs GLU (1.29×10^{-3}), and vs L-SER (2.78×10^{-5}), proved that the sensor is selective versus AA, UA, GLU, and L-SER.

8.3.3. Analytical applications

Whole blood samples were obtained from the Universitary Hospital in Bucharest (Ethics committee approval nr. 65573/14.12.2018). The blood samples were analyzed as obtained directly from patients, without any pretreatment.

46
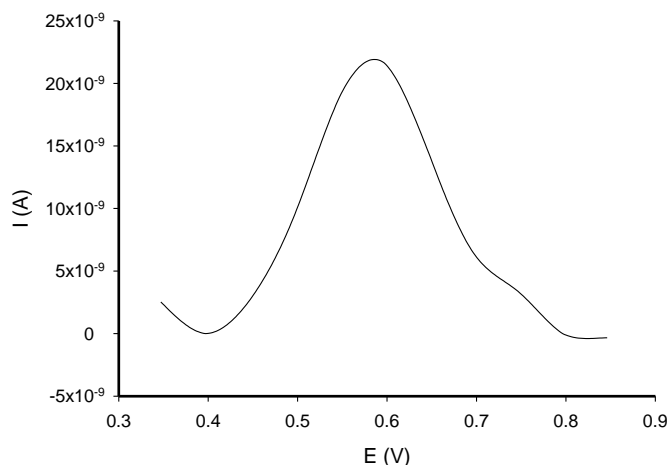
Figure 8.3. Example of voltammogram obtained for the assay of dopamine in whole blood samples.

The DPV technique was used to determine the dopamine in whole blood samples. The cell was filled with the whole blood sample and the peak height was measured. The unknown concentrations were determined from the calibration equation as described above.An example of voltammogram obtained using DPV for the assay of dopamine in whole blood samples is shown in Figure 3. The average recovery of dopamine in whole blood samples was 95.52% with RSD of 0.34% (N=5).

CONCLUSIONS

C1. General conclusions

Two 3D stochastic microsensors were designed for the simultaneously assay of levodopa and dopamine as biomarkers in the diagnosis of brain cancer, and also in the treatment of brain cancer. The wide linear concentration ranges, the limits of determination, selectivity and the high sensitivity of the proposed microsensors coupled with the high recoveries recorded for each microsensor allow the reliable molecular recognition and quantitative determination of levodopa and dopamine in biological samples such as whole blood, urine, and tumoral tissues. The addition of 1-adamantyloleamide to the AuNPs/MWNTs paste improved the response characteristics of the proposed 3D microsensors in terms of sensitivity and limit of quantification. Further, the proposed microsensors had lower limits of quantification, and wider linear concentration ranges for the

simultaneous assay of levodopa and dopamine, if compared with other sensors and methods reported to date.

A disposable stochastic sensor was designed for the fast screening of biological samples (whole blood, tissue samples) for three biomarkers: CEA, p53, and CA19-9. The high sensitivity, and selectivity, as well as the wide concentration ranges obtained for the assay of the three biomarkers recommend it for the screening tests of whole blood and tissues samples in order to be able to have a fast and early diagnosis of brain and gastric cancers.

A new needle stochastic sensor was designed for the assay of IL-1β , IL-6 and IL-12 as biomarkers for early diagnosis of brain cancer. The wide linear concentration ranges as well as the limits of determination allowed the assay of these interleukins in different types of biological samples like tumoral tissues, whole blood, and urine. The feature of the sensor and screening method is their utilization for early diagnosis of brain cancer.

The two stochastic microsensors based on immobilization of protoporphyrin IX in single and multi-walled carbon nanotubes decorated with Cu and Au nanoparticles designed for molecular recognition of IDH1 and IDH2 were reliable used for screening tests of biological samples (brain tumor tissue samples and whole blood samples). The highest sensitivity was recorded when the stochastic microsensor based on multi-walled carbon nanotubes decorated with Cu and Au nanoparticles was used.

Disposable stochastic sensor based on a nanofilm of a composite material comprising graphene nanoplatelet and silver particles deposited on silk, and modified with α-cyclodextrin was designed, characterized, and validated for the assay of HRG-α in biological samples. The proposed sensor exhibited high sensitivity and selectivity on a wide concentration range. The sensor had as features utilization in clinical laboratories and theatres for fast detection and quantification of HRG-α, in order to have a fast and early diagnosis of brain cancer, and of cancer metastasis.

Two 3D stochastic microsensors based on single and multiwalled carbon nanotubes modified with 2,3,7,8,12,13,17,18-octaethyl-21H,23H-porphine manganese (III) chloride were designed, characterized, and validated for the molecular recognition and quantitative determination of HGR-α in biological samples such as whole blood and tumoral brain tissue samples. The microsensors were highly sensitive and selective and show wide linear concentration range. They were validated versus ELISA with very good results. The features of the proposed 3D

stochastic microsensors is their utilization of fast screening tests performed by medical practitioners and in the surgery rooms to verify the state of health of the patients, and the progression of the brain tumor and the efficiency of the treatment.

An electrochemical sensor based on graphene paste modified with sulphur and protoporphyrin IX wasproposed for the assay of dopaminein whole blood samples. The electrochemical sensor exhibited high selectivity, low limits of detection and determination, and high sensitivity. The sensor was validated using whole blood samples.

C2. Original contributions

- The design of new stochastic and voltametric sensors for the analysis of specific cerebral tumors biomarkers
- Quantitative and qualitative detection of α-heregulin, IDH1 and IDH 2, dopamine, L-DOPA, IL6, IL12, IL β by using new 2D and 3D stochastic sensors
- New methods of screening for the early detection of cerebral tumors

C3. Perspectives for future developments

Implementation of sensors and screening methods in operating rooms and in the offices of family doctors and neurosurgeons to improve the health of patients.

References

1. Ostrom QT, Patil N, Cioffi G, Waite K, Kruchko C, Barnholtz-Sloan JS, CBTRUS Statistical Report: Primary Brain and Other Central Nervous System Tumors Diagnosed in the United States in 2013–2017, Neuro-Oncology, 2020; 22(Suppl. 1):iv1-iv96.

2. Ciurea AV(coord.), Tratat de neurochirurgie Vol. 1, Editura Medicală, 2010.

3. Gigliotti MJ, Hasan S, Karlovits SM, Ranjan T, Wegner RE, Re-Irradiation with Stereotactic Radiosurgery/Radiotherapy for Recurrent High-Grade Gliomas: Improved Survival in the Modern Era, Stereotact. Funct. Neurosurg. 2018; 96(5):289-295.

4. Stupp R, Brada M, van den Bent M J, Tonn J C, Pentheroudakis G, High-grade glioma: ESMO Clinical Practice Guidelines for diagnosis, treatment and follow-up, Ann. Oncol. 2014; 25(suppl 3):iii93-101.

5. Bailey P, Cushing H.: A classification of the tumors of the glioma group on a histogenic basis with a correlated study of prognosis. Lippincott, Philadelphia, 1926.

6. Arseni C, Carp N: Anatomia patologică a tumorilor sistemului nervos, Editura Didactică și Pedagogică - București, 1978.

7.   Louis DN, Perry A, et al. The 2021 WHO Classification of Tumors of the Central Nervous System: a summary, Neuro-Oncology, 2021, 23(8):1231–1251.

8.   Greenberg MS (coord), Handbook of neurosurgery, 9th edition, Thieme, 2020 pg.595

9.   Jelski W, Mroczko B, Molecular and circulating biomarkers of brain tumors, Int. J. Mol. 2021, 22, 7039.

10.   Staedtke V, Dildar a Dzaye O, Holdhoff M, Actionable molecular biomarkers in primary brain tumors, Trends Cancer. 2016; 2(7): 338–349.

11.   El-Jawahri A, Patel D, Zhang M, Mladkova N, Chakravarti A, Biomarkers of clinical responsiveness in brain tumor patients: progress and potential, Mol Diagn Ther. 2008;12(4):199-208.

12.   Siegal T, Clinical Relevance of Prognostic and Predictive Molecular Markers in Gliomas, Adv Tech Stand Neurosurg. 2016;(43):91-108.

13.   Takahashi Y1, Nakamura H, Makino K, Hide T, Muta D, Kamada H, Kuratsu J, Prognostic value of isocitrate dehydrogenase 1, O6-methylguanine- DNA methyltransferase promoter methylation, and 1p19q co-deletion in Japanese malignant glioma patients, World J Surg Oncol. 2013; 11:284.

14.   Parsons DW, Jones S, Zhang X, et al. An integrated genomic analysis of human glioblastoma multiforme. Science. 2008; 321(5897):1807–12.

15.   Mardis ER, Ding L, Dooling DJ, et al. Recurring mutations found by sequencing an acute myeloid leukemia genome. N Engl J Med. 2009; 361(11):1058–66.

APPENDIX 1

LIST OF INTERNATIONAL AND NATIONAL CONFERENCES PRESENTATIONS

ORAL PRESENTATIONS

1. Disposable stocahstic sensor based on deposition of a nanolayer of silver on silk for molecular recognition of specific biomarkers, **Sorin Sebastian Gheorghe**, RI Stefan-van Staden, RM Ilie-Mihai, M Badulescu, XXVIth International Symposium on Bioelectrochemistry and Bioenergetics, Cluj-Napoca, Romania, 9-13 Mai 2021

2. 3D stochastic sensors as new tools for early diagnosis of brain cancer, RI Stefan-van Staden, **Sorin Sebastian Gheorghe**, C Cioates Negut, ACS Fall 2021, Atlanta, USA, 22 – 26 August, 2021.

3. Validation of a Screening Method based on a Needle Stochastic Sensor for the Determination of Interleukins 1β, 6, and 12 in Biological Samples, **Sorin Sebastian**

Gheorghe, RM Ilie-Mihai, RI Stefan-van Staden, A Bratei, Eurachem Virtual Scientific Workshop, 14-15 Iulie, 2020

APPENDIX 2

PUBLISHED ISI ARTICLES

1. C. Cioates Negut, **Sorin Sebastian Gheorghe**, R. I. Stefan-van Staden, J. F. van Staden, Fast screening test for molecular recognition of levodopa and dopamine in biological samples using 3D printed stochastic microsensors, Journal of Pharmaceutical and Biomedical Analysis, 2021, 205:114292; https://doi.org/10.1016/j.jpba.2021.114292 **(IF: 3.209)**

2. RM Ilie-Mihai, **Sorin Sebastian Gheorghe**, RI Stefan-van Staden, A Bratei, Electroanalysis of Interleukins 1 β, 6, and 12 in Biological Samples Using a Needle Stochastic Sensor Based on Nanodiamond Paste, Electroanalysis 20210, 33:6-10; https://doi.org/10.1002/elan.202060118; **(IF: 3.223)**

3. RI Stefan-van Staden, C Cioates Negut, **Sorin Sebastian Gheorghe**, A Ciorita, 3D stochastic microsensors for molecular recognition and determination of heregulin-α in biological samples, Analytical and Bioanalytical Chemistry, 2021, 413:3487-3492, https://doi.org/10.1007/s00216-021-03295-7 **(IF:4.142)**

4. RI Stefan-van Staden, **Sorin Sebastian Gheorghe**, RM Ilie-Mihai, M Badulescu, Disposable Stochastic Sensor Based on Deposition of a Nanolayer of Silver on Silk for Molecular Recognition of Specific Biomarkers, Journal of The Electrochemical Society, 2021, 168(3):037515; https://doi.org/10.1149/1945-7111/abeea2 **(IF:4.316)**

5. **Sorin Sebastian Gheorghe**, C Cioates Negut, M Badulescu, RI Stefan-van Staden. Sensitive Detection of Heregulin-α from Biological Samples Using a Disposable Stochastic Sensor Based on Plasma Deposition of GNPs–AgPs' Nanofilms on Silk. *Life*. 2021; 11(9):894. https://doi.org/10.3390/life11090894 **(IF: 3.817)**

6. **Sorin Sebastian Gheorghe**, RM Ilie-Mihai, RI Stefan-van Staden, Determination of Dopamine in Whole Blood Samples Using A New Electrochemical Sensor Based on Graphene, **UPB Sci Bull, Acceptată. (IF: 0.49)**

7. C. Cioates Negut, R. I. Stefan-van Staden, **Sorin Sebastian Gheorghe**, M. Badulescu, Stochastic Sensors for the Molecular Recognition and Determination of Heregulin-α in

Biological Samples - oral presentation (051), in Proceedings of the 7th International Conference on Sensors Engineering and Electronics Instrumentation Advances (SEIA' 2021), 22-24 September 2021, Palma de Mallorca, Mallorca (Balearic Islands), Spain, pp. 150-151, ISBN: 978-84-09-33525-1.

Cumulated IF: 19.197

ARTICLES SENT FOR PUBLICATION

1. RI Stefan-van Staden, C Cioates Negut, **Sorin Sebastian Gheorghe**, P Sfarloaga, Stochastic microsensors based on carbon nanotubes decorated with Cu and Au nanoparticles, for molecular recognition of isocitrate dehydrogenases 1 and 2 in biological samples

APPENDIX 3

ABBREVIATIONS

2-HG= 2-hidroxiglutarat

AA= Ascorbic acid

DNAtc= circulating tumoral DNA

AOA= 1-adamantyloleamide

mRNA= messenger RNA

miRNA= MicroRNA

AuNPs = Gold nanoparticles

CA19-9= Carbohydrate antigen 19-9

CEA= Carcinoembryonic antigen

cfDNA= circulating free DNA

CL= Chemiluminescence

cmfiRNA= circulating free microRNA

CNT= Carbon nanotubes

CSC= Cancer Stem Cells

CT= Computer tomography

CTC= Circulating Tumor Cells

DA= Dopamine

ECL= Electrochemiluminescence

EEG= Electroencephalography

EGFR= Epidermal growth factor receptor

FGF-2= Fibroblast growth factor 2

FTIR= Fourier-transform Infrared Spectroscopy

GBM= Glioblastoma multiforme

GFAP= Glial fibrillar acid protein

GLU= Glutamine

HGG= High-grade Glioma

HPLC= High performance liquid chromatography

HRG= Hereguline

ICE= Interleukin conversion enzyme

IDH= Isocitrate dehydrogenase

IL-1ra= Interleukin 1 antagonist receptor

IL-2= Interleukin 2

MRI= Magnetic Resonance Imaging

CSF= cerebrospinal fluid

L-dopa= Levodopa

LGG= Low grade glioma

L-SER= L-serine

MGMT = Methylguanine methyltransferase

MMPs = Matrix metalloproteinases

MWNTs = Multiwalled nanotubes

NADPH = Nicotinamide adenine dinucleotide phosphate

nDP= Nanodiamond paste

PC= Circulating proteins

PEC= Photoelectrochemical

PET-CT= Positron emission computer tomography

PIX= Protoporphyrin IX

PL= Photoluminescence

RRS= Rayleigh dispersion

SERS= Surface enhanced Raman spectroscopy

CNS= Central nervous system

SPS= Solid Phase Spectrophotometry

TGFb= Transforming growth factor beta

TIMPs= Tissular inhibitors of metalloproteinases

TNFa= Tumor necrotizing factor alpha

UA= uric acid

VE= Extracellular vesicles

VEGF= Vascular endothelium growth factor

α-CD= α-cyclodextrin

α-KG= α-ketoglutarate